

Microfabrication Technologies in Dielectrophoresis Applications – a review

Rodrigo Martinez-Duarte

Laboratory of Microsystems(LMIS4), École Polytechnique Fédérale de Lausanne, Switzerland

Keywords: Microfabrication, Dielectrophoresis, technology, metal electrode, insulator-based, contactless, carbon electrode, PDMS, electrodes, high throughput, 3D

Abbreviations: **DEP** dielectrophoresis, **EOF** electroosmotic flow, **AFM** atomic force microscopy, **PDMS** polydimethylsiloxane, **CMOS** complementary metal-oxide semiconductor, **PCB** printed circuit board, **iDEP** insulator-based DEP, **eDEP** electrodeless DEP, **PMMA** polymethylmethacrylate, **PC** polycarbonate, **CarbonDEP** carbon-electrode DEP, **PSA** pressure-sensitive double-sided adhesive, **cDEP** contactless DEP, **RIE** reactive ion etching, **PBS** phosphate buffered saline, **DLP** digital light processor, **DMD** digital micromirror device, **LCD** liquid crystal display, **PEDOT:PSS** Poly(3,4-ethylenedioxythiophene) poly(styrenesulfonate)

*Corresponding Author: Rodrigo Martinez-Duarte

Laboratory of Microsystems (LMIS4), École Polytechnique Fédérale de Lausanne

BM3124 Station 17

CH-1015 Lausanne, Switzerland

Email: drmartz@gmail.com

Phone number: +41216936582

Fax: +41216935950

Abstract

Dielectrophoresis (DEP) is an established technique for particle manipulation. Although first demonstrated in the 1950s, it was not until the development of miniaturization techniques in the 1990s that DEP became a popular research field. The 1990s saw an explosion of DEP publications using microfabricated metal electrode arrays to sort a wide variety of cells. The concurrent development of microfluidics enabled devices for flow management and better understanding of the interaction between hydrodynamic and electrokinetic forces. Starting in the 2000s alternative techniques have arisen to overcome common problems in metal-electrode DEP, such as electrode fouling, and to increase the throughput of the system. Insulator-based DEP and light-induced DEP are the most significant examples. Most recently, new 3D techniques such as carbon-electrode DEP, contactless DEP and the use of doped PDMS have further simplified the fabrication process. The constant desire of the community to develop practical solutions has led to devices which are more user friendly, less expensive and are capable of higher throughput. The state-of-the-art of fabricating DEP devices is critically reviewed in this work. The focus is on how different fabrication techniques can boost the development of practical DEP devices to be used in different settings such as clinical cell sorting and infection diagnosis, industrial food safety and enrichment of particle populations for drug development.

1. Introduction

Dielectrophoresis is a well-known particle manipulation technique that takes advantage of the interaction of polarizable matter with non uniform electric fields. The most important requirement for this technique is the implementation of an electric field gradient which induces a dipolar moment on the particle of interest. The stronger the gradient, the stronger the dipole is and therefore the stronger the DEP force actuating on the particle. The direction of the force, either towards to the field gradient as in positive DEP or away from it as in negative DEP, is given by the difference in complex permittivity between the particle of interest and the suspending media. The technique was first described by Pohl in the 1950s [1]. The great potential of the technique to selectively manipulate targeted particles was well realized then but it was not until the establishment of miniaturization techniques in the 1990s that DEP became a popular research field. The use of microfabrication techniques allowed for the positioning of electrodes very close to each other, by tens of micrometers, and therefore the use of practical voltages, tens of volts, instead of thousands of volts required in the initial experiments where electrodes were separated by centimeters. The 1990s saw an explosion of DEP publications, mainly from the groups of Pethig, Gascoyne, Fuhr and Morgan and Green who used metal microelectrodes to sort a wide variety of cells as reviewed a number of times before [2, 3]. The development of microfluidics also allowed for the creation of better devices for flow management and better understanding of the interaction between hydrodynamic and electrokinetic forces. Starting in the 2000s alternative techniques started to arise to overcome common problems in metal-electrode DEP, such as electrode fouling, and/or to increase the throughput of the system. Insulator-based DEP and light-induced DEP are the most significant examples; carbon-electrode DEP and contactless DEP became active after 2005 and more groups are starting to use them. Most recently, the use of doped PDMS (polydimethylsiloxane) as electrode material was demonstrated. The development of these new techniques and the constant desire of the community to develop practical solutions have led to devices which are more user friendly, less expensive and are capable of high throughput. Although the biggest impact of DEP has been widely positioned in the manipulation of cells and biological matter for health care applications, DEP also shows great potential in other applications including environmental [4]

and energy; in nanowire sorting [5] and manipulation [6]; to improve AFM (atomic force microscopy) probes [7]; and to obtain re-configurable optical waveguides [8]. In general, any application that can benefit from the non-contact manipulation of micro- and meso-scale objects can be positively impacted by DEP. The purpose of this work is to review the current literature on the different microfabrication techniques to make DEP devices for batch manipulation of particles. Although some of his fabrication techniques can also be used for single particle manipulation, single cell analysis and molecule [9] techniques including DEP cages [10] and the most recent work in DEP-enabled micromanipulators [11] is not reviewed here. DEP theory and applications are also not reviewed here given the significant number of very good reviews already available [2, 3, 12-17]. In the current work, an overview of each fabrication process is presented followed by an assessment of the technique in terms of material and infrastructure cost and other parameters. The focus is on how different fabrication techniques can boost the development of devices to allow DEP to become a more practical tool in different settings, for example: in clinical cell sorting to provide a less expensive alternative to fluorescence-activated cell sorting (FACS[®]) or magnetically-activated cell sorting (MACS[®]); in industrial food safety to quickly identify threats, *i.e.* *E.coli* and *salmonella*, with very high sensitivity; in hospitals to quickly pinpoint the cause of an infection; in drug development to enrich very large populations of particles of interest.

2. Theory Background

A theoretical treatment of the DEP force is not the focus of this paper. However, the governing equations are briefly presented to introduce the concepts of positive and negative DEP and illustrate how DEP can selectively trap or repel targeted particles. The hydrodynamic drag force and the continuity equations are also presented to explore their interaction with the DEP force towards facilitating high throughput devices.

The dielectrophoretic force F_{DEP} is given by:

$$F_{DEP} = 1/4vRe[\alpha]\nabla E_{rms}^2 \quad (1)$$

where v is the volume of the particle to be manipulated and α is its effective polarisability. In the case of a spherical particle of radius r in a medium m equation 1 becomes:

$$F_{DEP} = 2\pi\epsilon_m r^3 Re[f_{CM}]\nabla E_{rms}^2 \quad (2)$$

With the real part of the Clausius-Mossotti (CM) factor, $Re[f_{CM}]$, defined as

$$Re[f_{CM}] = \frac{\frac{\epsilon_p^* - \epsilon_m^*}{\epsilon_p^* + 2\epsilon_m^*}}{\epsilon_p^* + 2\epsilon_m^*} \quad (3)$$

where r denotes the radius of the particle, $|\nabla E|$ the magnitude of the electric field gradient, ϵ_p^* the complex permittivity of the particle and ϵ_m^* of the media. Complex permittivity ϵ^* is given by:

$$\epsilon^* = \epsilon - \frac{j\sigma}{2\pi f} \quad (4)$$

and depends on the permittivity ϵ and conductivity σ of the particle or the media and the frequency f of the applied electric field. The imaginary number $\sqrt{-1}$ is represented by j . A non-uniform electric field is necessary to induce a DEP force as stated in eqn. 1 (otherwise $\nabla E = 0$). Positive values of $Re[f_{CM}]$, see equation 3, denote the induction of a positive DEP force that causes a particle to trap within regions of high electric field magnitude. Negative values of $Re[f_{CM}]$ denote negative DEP which means particles move towards regions of low or no electric field. The magnitude of the induced DEP force, either positive or negative, on a particle with fixed radius r is proportional to the absolute value of $Re[f_{CM}]$ and the magnitude of the electric field gradient squared. Since the magnitude of the DEP force depends on the electric field and this in turn is inversely proportional to the distance between electrodes; narrow gaps are desired to minimize the voltage needed to create a suitable field gradient for DEP, as long as they do not represent a physical trap to the particles.

The hydrodynamic drag force acting on a particle in a channel featuring laminar flow is given by the Stokes drag force:

$$F_{drag} = -bV \quad (5)$$

Where b is a factor depending on the dimensions of the particle and the properties of the fluid and V is the velocity of the particle which is given by the velocity of the fluid. In the case of a spherical particle:

$$F_{drag} = 6\pi\mu rV \quad (6)$$

Where μ is the viscosity of the media and r is the radius of the particle. The continuity equation establishes that the mass flow rate Q in a micro-channel equals the product of the flow velocity V and the cross-section area A of the channel

$$Q=VA \quad (7)$$

therefore, for a fixed linear velocity the mass flow rate can be increased simply by increasing the cross-sectional area. Since the hydrodynamic drag force acting upon particles flowing in a micro channel depends on the flow velocity, the maintenance of low flow velocity in the channel leads to a hydrodynamic force that can be easily overcome by a DEP force created using practical voltages and electrode gaps. Once the channel cross-section is increased one needs to induce an electric field throughout the whole volume of the channel to guarantee all particles flowing through get influenced by a DEP force. Since taller, rather than wider, channels are desired to maintain a small footprint of the DEP chips and minimize costs; the use of 3D electrodes, as tall as the channel and contained inside the channel, enables the addressing of all particles flowing in the channel. This is in contrast to planar electrodes positioned on the channel floor or ceiling which only enable addressing those particles flowing close to the channel surfaces. Although gravity does act on the particles, its effect is considered negligible in high throughput systems since the particle flows through fast enough to prevent sedimentation as detailed by Martinez-Duarte *et al* [18].

3. Fabrication parameters to consider towards practical applications

The factors of importance considered here are cost of the required infrastructure for fabrication, fabrication time and complexity, material cost, capability to resolve small gaps between electrodes and potential to fabricate 3D structures. It is assumed that all microfabrication processes detailed here, or at least part of a specific process, are conducted in a cleanroom and thus the cost of running a cleanroom is not considered. An ISO 6 cleanroom should be enough to guarantee useful DEP devices. Experimental advantages and disadvantages of each kind of DEP devices are also discussed. The cost of the material itself, the infrastructure required for fabrication and the fabrication time and complexity are important parameters to assess the feasibility to produce disposable devices. It is important to note that while disposable devices are required for some applications, especially in health care to avoid sample contamination, they may not be required in other applications such as the food industry, nanowire manipulation and

environment monitoring. However, the cost of the devices still must be low to allow DEP to impact the highest number of application. Besides low cost, the devices must be robust, user-friendly and achieve highly reproducible results. Another constraint in the fabrication of DEP devices comes from the fact that electric field gradient is inversely proportional to the distance between electrodes, therefore to induce electric field gradients suitable for DEP using practical voltage levels, on the order of tens of volts, the gap must be optimized to the size of particles intended to be manipulated. In the case of biomolecules, such as DNA and proteins, very small gaps, in the order of few micrometers, are desired. Fabrication constraints are high in this case since many low cost techniques are not able to resolve very small gaps, especially between 3D structures. If one intends to manipulate cells, the gap between electrodes must be increased to tens of micrometers thus reducing constraints on how small of a gap must be fabricated with a specific technique. Many low cost techniques are able to resolve the gaps needed, even between 3D structures, for cell and bacteria manipulation. From the experimental point of view, small gaps between electrodes are desired to minimize the voltage needed to create a DEP force. Except for metal-electrode DEP, all other techniques make use of voltages above 10 V_{pp} . This is because the electrodes, micro or macro-sized, are either far apart, are not made from an ideal conductor or are covered by a protective polymer coating. If the required voltage is above 20 V_{pp} the need for a voltage amplifier, DC or RF, additional to the function generator sometimes appears since current commercial generators are usually limited in their voltage output to 20 V_{pp} . The benefit of using 3D electrodes has been detailed in the theory section. 3D electrodes may not be needed in all applications but they are expected to significantly impact the performance of devices in high throughput applications.

4. Metal-electrode

The bulk of the research work performed to this date on DEP has been done using metal electrodes. Pohl and colleagues conducted a very significant amount of work starting in the 1950s [1, 19-31] using simple wire and metal foil or plates as electrodes. The separation between these metal macro electrodes was in the order of centimeters and the arrangement was usually embedded in a chamber in which the sample was deposited. Hundreds of volts were required to polarize the device. The sample chamber was as simple as a polymer ring topped with a glass slide. The advent of microfabrication techniques eventually led to the use of metal

microelectrode arrays to implement DEP. To the best of the author's knowledge, the paper published by Price *et al* in 1988 [32] is the first demonstration of such device. A seed layer of chrome was first sputtered on a glass substrate followed by a 1 μm -thick sputtered layer of copper. These layers were then patterned by wet etching using a polymer mask and such pattern is finally covered with a 200 nm layer of chemically deposited gold. In such way intercastellated electrode arrays with mean spacing between electrodes of 60 μm were fabricated. The behavior of test particles under DEP forces, implemented by polarizing the array by mere 10 V_{pp} , instead of hundreds or thousands of volts as before, was monitored using optical absorbance at 450 nm. This was the beginning of a revolution that led to many milestones in DEP-based particle manipulation using planar metal electrodes.

4.1 2D Metal micro-electrodes

The fabrication details of planar metal electrodes, and their use, have been reviewed before [2, 3] and are therefore out of the scope of this review. However, the techniques used for the fabrication of such electrodes are detailed next to build a base from where to start unfolding the development of microfabrication techniques for DEP devices. The fabrication of planar metal electrodes mainly requires for metal deposition, polymer patterning and etching infrastructure. A variety of metals can be deposited on a substrate using currently common equipment in a microfabrication facility: electron beam evaporation or sputtering. Two different alternatives are usually followed to pattern a metal layer: lift-off or wet/dry etching. In the case of lift-off, a polymer topography is first fabricated on the substrate, usually glass or silicon, using standard photolithography. Metal is then evaporated on the whole substrate such that metal is only directly deposited on the substrate on those areas not covered by the polymer topography. The metalized substrate is then dipped in a chemical to dissolve the polymer topography consequently lifting-off any metal deposited on it. In the case of wet or dry etching the metal is first evaporated or sputtered on the entire substrate. It is only after metal deposition that a polymer mask is patterned on the metal using photolithography. The openings in the polymer topography grant direct access to etch the metal either by wet or dry techniques. After etching, the polymer is dissolved to reveal the underlying metal pattern. Alternatively, a metal layer can be directly patterned using laser ablation or ion-milling or the metal can be deposited through a stencil, or shadow mask. In such cases, polymer photolithography and etching are not necessary but the cost of laser ablation or ion-milling machines must be added. If using a stencil, the

fabrication cost of a working stencil must be added [33]. Several metals have been used in DEP applications but gold and platinum remain the top choices given their proven biocompatibility and electrochemical stability. Indium tin oxide (ITO), a transparent conductor when used in thin layers, is also common to pattern microelectrodes following techniques similar to those used for metals. A variety of electrode designs including castellated, serrated, spiral, saw tooth have been used by different groups. Mature and industrial technologies such as CMOS (complementary metal-oxide semiconductor), a fabrication process widely used in the integrated circuit industry, has also been used to implement dynamic DEP traps thanks to a matrix of several individually addressable electrodes [34-36]. Although a wide variety of particles have been manipulated using planar electrodes ranging from nanowires to mammalian cells, the throughput achieved using such devices is commonly not sufficient to enable the use of DEP in a practical setting, for example in the clinic or industrial-level manufacturing.

One of the main reasons for this is that polarization of the electrode array only creates field gradients close to the surface of the electrodes. Although this fact holds for most electrodes, 2D or 3D, planar electrodes are usually fabricated on the bottom of the channel and thus an electric field gradient is only effectively established in sample volumes less than $\sim 30 \mu\text{m}$ away from the bottom. Particles flowing beyond such limit do not experience any DEP force thus lowering the efficiency of the system. Another reason for low throughput is the cross-section of the channels commonly used in microfluidics. A small channel cross-section inherently restricts how much fluid can flow through the channel per unit of time using normal pressures. One of the most straight forward ways to increase throughput is to increase the channel cross section either by making it wider, taller, or both. Taller channels are usually preferred to keep the footprint of the DEP device small. Planar electrodes do not perform well in tall channels. Consequently, the need to maximize the DEP forces present throughout the bulk of taller channels has led to new approaches in electrode design. An immediate improvement was the fabrication of planar electrodes on both the floor and the ceiling of the channel. For example, Fuhr and colleagues developed an exciting device [37-39] where the introduction of top and bottom electrodes lead to the implementation of several manipulation functions, even feasible for single cell studies, within a single channel such as: deflection, focusing, pairing, trapping (using an octopole configuration) and electrofusion as shown in Figure 1. In their case, channel heights of around $40\text{-}50 \mu\text{m}$ were used such that the electric field gradient generated by top and bottom electrodes exists

throughout the bulk of the channel. However, as channel height increases beyond 50 μm particles flowing in the middle of the channel may not experience any DEP force at all, neither induced from the bottom or top electrodes.

4.2 3D metal electrodes

Voldman and colleagues [40] introduced the use of electroplating to fabricate extruded gold electrodes inside the channel volume and not on its surfaces. Electroplating is a process in which metal ions in a solution are moved by an electric field to deposit on an existing metal layer. Electrodeposition and thick film photolithography must be added to the fabrication process of metal planar electrodes if fabricating volumetric metal structures. In this case the process usually starts with the patterning of a seed layer using thin film fabrication. A template as thick as the targeted height of the pattern is then fabricated around the seed layer to contain the electroplated metal. This template is usually made out of a polymer using thick film photolithography and its fabrication can be challenging. High aspect ratio gaps between the electrodeposited structures require the fabrication of thin walls in the polymer template with very high aspect ratio which can compromise their mechanical stability. Voldman *et al* fabricated 60 μm -high electrodes contained in a 150 μm channel. The metal pillars were arranged in a quadrupole configuration (Figure 2 left) to establish a DEP-based trap for single cells. In such way they implement an interrogation site for flow cytometry applications which maintains the cell securely in place even against disturbing flows [40]. Wang *et al* later also electroplated gold structures and embedded them in the walls of a microchannel. Such electrodes span the entire height of the channel walls, 30 to 40 μm , which enabled the dynamic positioning of a stream of particles anywhere along the width of the channel in a technique they called lateral flow DEP [41-43]. The use of two different frequencies to independently polarize these electrodes embedded on each side of the channel led to a complete purification of a cell sample from latex beads [43].

Other 3D approaches involving metal electrodes are those from Fatoyinbo *et al*, Park *et al* and Abidin *et al*. Although not technically microfabricated, they are important to mention because they illustrate alternative, and ingenious, methods to fabricate DEP devices without the need for complex infrastructure. Fatoyinbo and colleagues first built a sandwich of intercalated layers of aluminum foil and epoxy resin film. Drilling holes through this stack automatically created ring electrodes distributed all along the walls of the drilled holes. The DEP behavior of yeast cells was quantified by measuring the optical absorbance at the center of the well; absorbance

increases when negative DEP clusters the cells away from the walls, and decreases when cells are attracted to the walls of the well [44]. Park and Madou fabricated a DEP separation chamber using a pair of polished stainless steel wires (1.58 mm diameter), PDMS and silicone. The wires are spaced from each other approximately 250 μm using a stack of Scotch[®] tape pieces. The pair is then positioned in the middle of a fluidic chamber fabricated in PDMS and the whole arrangement is sealed shut using silicone. The device is demonstrated by filtering carbon nanofibers from canola oil [45]. Abidin and colleagues demonstrated trapping of yeast cells in a DEP device featuring a composite mesh made by weaving stainless steel wire and polyester yarn cloth together [46]. The 100 μm -diameter metal wires are kept parallel, 150 μm apart, using the polyester yarn and are connected such that no adjacent wires have the same polarity. After weaving, individual pieces of such composite cloth (around 3 X 4 cm) are alternately stacked with PMMA (polymethylmethacrylate) spacers. The device is closed on both ends by PMMA plates to create a 14 ml fluidic chamber. Trapping of yeast with more than 85% efficiency at flow rates up to 500 $\mu\text{l}/\text{min}$ is demonstrated using voltages as low as 30 V and frequency of 1 MHz [46].

The use of metal microelectrodes for DEP came as a natural non-conventional application of the rapidly evolving field of integrated circuits. As the world embraced digital technologies the expertise to fabricate metal planar electrodes rapidly evolved, the cost of manufacturing decreased and the technology became readily available. Indeed, the main advantage of using 2D metal-electrode DEP is that the fabrication techniques are so developed that high fabrication yield of a myriad of designs is possible, including those featuring very narrow gaps between electrodes. A clear example of this is the use of CMOS technologies to mass fabricate DEP cages. The chips can be outsourced to a foundry and because CMOS is so widely used the price can be minimized. However, the chips still contain precious metal which makes them unlikely to be disposable. Furthermore, in order to make such chips suited for DEP experimentation some backprocessing is needed thus adding to the cost and complexity of the process. Conventional metal patterning techniques are by far more used by the community since cleanrooms, from the very basic to cutting-edge ones, are now widely available and the device can be manufactured in house (instead of being fabricated at a foundry). In such cases the fabrication time can be as quick as few hours and still fairly narrow gaps, $>1 \mu\text{m}$, can be fabricated when using standard photolithography techniques. This limit on the achievable gap size can be extended to the

nanometer scale only if using e-beam or laser writers to pattern the polymer mask, or when using laser ablation or ion-milling to directly pattern the metal layer. In the case of direct patterning, fabrication costs are lowered since no polymer mask nor metal etching are needed. However, such direct patterning equipment is at this time expensive and requires constant maintenance and technical training to run properly. The cost of a metal evaporator or sputter is well into the tens of thousands of dollars. E-beam writers and ion-based millers surpass the hundreds of thousands. Although standard polymer photolithography equipment such as spin coater, hotplates and chemical benches can be a few thousands of dollars altogether, the addition of a mask aligner raises the bill for a couple hundred more thousand dollars. But most importantly, gold and platinum are expensive materials. The material cost may not be a factor in the case of planar electrodes, where usual thickness is a couple of hundred of nanometers, but can be when using electroplated electrodes with thickness well into the tens of micrometers. Moreover, the patterning of metals usually requires the use of polymer sacrificial layers. Positive resists are widely used, and relatively inexpensive, to pattern planar electrodes. Negative resists, such as SU-8, are a bit more expensive and are mostly used to fabricate a mold for electroplating. Dry film resists, such as ORDYL®, instead of liquid-base photoresists may also be used during the process to replace the need for a spin coater with a need for a laminator which is usually cheaper and easier to maintain.

The biggest advantage of using metals is that only a few volts are needed to induce DEP on a sample. A battery and low cost electronics could be used to implement a handheld, point-of-care device based on DEP, a fact that cannot be easily said for many other DEP techniques. If voltage levels above 20 V_{pp} are needed, more expensive and bulky electronics including a DC or a RF amplifier will be required. The reason only a few volts are needed in metal-electrode DEP is that the electrodes are in contact with the sample, and unfortunately that is also one of the main disadvantages of metal electrodes. Under experimental conditions, metal electrodes can interact with the sample which leads to sample electrolysis, bubbling and electrode arcing which reduces the lifetime of the device [47]. Electrode reactions are more likely to happen at low frequencies, high media conductivities and high voltage and after knowing the limits of a particular design, the sample conductivity and experimental protocol can be tailored accordingly. Manipulation of cells can be effectively done using high frequencies in the hundreds of kHz to MHz range [12] but the manipulation of bioparticles has mostly been in the DC or low kHz range [13]. To

ameliorate this problem, metal electrodes could be coated with a very thin layer of inert polymers, such as parylene, to prevent interaction with the sample. If using such approach, the material cost of the electrodes can be drastically decreased since noble metals are no longer needed. On the other hand, a few approaches to re-use metal electrodes have been implemented. One example is the use of copper electrodes patterned on a printed-circuit board (PCB) and interfaced to the sample using a thin cover glass slip [48]. In this case the electrodes can be inexpensive and re-usable, the chance for electrode reaction with the sample is eliminated, and a cheap, disposable device can be used to process the sample; but significant more voltage is needed to induce a DEP force on the sample through the glass layer. Those authors demonstrated manipulation of latex beads and HeLa cells using a sinusoidal signal with 1 MHz frequency and voltages in the range between 75 and 80 V_{pp} (using a RF amplifier).

5. Doped Silicon

Another approach to minimize electrochemical interaction between the sample and the electrodes is to use doped silicon as the electrode material. Iliescu and colleagues fabricated DEP devices where 3D electrodes also form the channel walls. They demonstrated a number of designs for cell manipulation [49-52]. The device (Figure 3) is made of three parts: a thick, heavily doped silicon layer, containing the microfluidics channel and the electrodes, which is sandwiched in between a couple of glass dies anodically bonded to the silicon layer. The channel inlet and outlet are drilled in one of the glass dies. The fabrication process includes glass drilling, anodic bonding, deep Reactive Ion Etching (RIE), glass thinning, fabrication of via holes and metallization leads. A P-type, heavy doped silicon wafer, with resistivity in the range between 0.001 and 0.015 $\Omega \cdot \text{cm}$ and thickness of 100 μm , is first anodically bonded to a Pyrex[®] glass wafer at 305 °C, 1000 V and 1000 mbar. A polymer mask is then fabricated on the silicon to define the pattern to etch in the next step. Channels and electrodes are then etched through the silicon layer using deep RIE, also known as the Bosch process, using a stop-etch on the glass die. After removal of the polymer mask, a second glass wafer with holes previously drilled using a diamond bit, is anodically bonded at 450 °C, 1500 V and 2000 mbar to seal the channel. An increase of temperature in this second bonding step was needed due to the low conductivity of the glass wafers with the silicon layer. The increased voltage and contact force were applied to increase the electrostatic force and achieve a better contact between the wafers. The bottom glass

wafer, the one which is not drilled, is then thinned to facilitate the fabrication of via holes to connect the silicon layer to a function generator. After protecting all other surfaces of the wafer-sized arrangement using wax, the device is dipped in a HF (49%)/HCl (37%) 10:1 solution until the thickness of the bottom glass is reduced from 500 μm to 100 μm . Metal (Cr + Au) is then deposited on the glass followed by the fabrication of a polymer mask to enable patterning of the metal using wet etching. The resulting metal mask enables the patterning of via holes to the silicon through the glass by dipping the arrangement in the HF/HCl solution again. After the holes are fabricated, the metal mask is removed by dipping in Cr and Au etchants. The final step of the process is the fabrication of metal leads to connect the silicon electrodes to the function generator. Chromium and gold are then again deposited on the bottom glass wafer and the connection leads are patterned using a polymer mask and wet etching. The polymer mask is finally removed to end the fabrication process. A finished device is shown in Figure 3.

The authors claim that their fabrication process first minimizes interaction of the sample with the electrodes, second readily achieves 3D electrodes spanning the whole height of the channel and third the device does not suffer from sample leakage since it is fully enclosed in a monolithic device. This last fact is very beneficial in the use of this device for high throughput systems since implementing high flow rates and pressures in the channel do not cause leakage in the microfluidic network, as it is often the case when using other materials/fabrication techniques. The device can be operated with voltages between 13-25 V_{pp} which can be implemented using a function generator, although one towards the high end of the ones currently available due to the voltage requirements. A further advantage is that silicon and glass are both inert and well characterized which is beneficial towards getting reproducible results. However, the fabrication process is fairly complex and requires relatively expensive infrastructure including RIE and metal deposition [49].

6. Insulator-based Dielectrophoresis

A well established alternative to metal microelectrodes is to use arrays of insulator structures to locally distort an otherwise uniform electrical field. In this technique, known as electrodeless (eDEP) or insulator-based dielectrophoresis (iDEP), metal macro electrodes, for example extruded wire rods or machined metal plates, are used to create a uniform electric field across an array of insulator structures. The presence of the insulator structures distorts the field and creates

field gradients. The big advantage is that the need for micro electrodes disappears thus reducing both the cost of the device itself and its fabrication. However, the name electrodeless DEP is misleading since electrodes are still needed. Insulator-based DEP is therefore preferred. A voltage as high as hundreds of volts, sometimes a few thousands, is commonly required since the macro-scaled electrode are now separated by millimeters, even a few centimeters. However, the bulk of the sample is not in contact with the electrodes and thus electrode fouling and sample electrolysis in the DEP-active area, common to metal micro electrodes, can be largely avoided. Various approaches have been used to implement this technique and are detailed next:

6.1 Insulator matrices

In this technique a channel is filled with dielectric beads, or other shapes such as rods, to achieve packing, and void spaces, at different degree. Other continuous matrices such as ceramic wool and textiles can be used. A uniform electric field is implemented across the matrix to create high electric field gradient volumes around the surfaces of the beads, and especially in the contact points between them, and lowest gradient in the gaps in between them (Figure 4). It can be viewed as a DEP-boosted physical filter which can also be re-usable. The constraint on pore size and uniformity is not as strict since the trapping is made by DEP forces and not purely by physical constriction; and since the previously trapped particles can be released by either turning the field off or by changing its frequency such that particles are repelled from the matrix surfaces, it can be cleaned and re-used. The electric field gradient is inversely proportional to the size of the particles with small particles leading to higher field gradients. Pioneering work is that from 1982 by Jin and Benguigui [53, 54] who studied the packing optimization based on the geometry of the beads and used it to fabricate different matrices to create an active filter. For example, they used 6 mm diameter glass beads packed in between concentric electrodes which were used to trap or repel magnesium oxide, polyvinylchloride, alumina, ilmenite and copper particles suspended in mixtures of kerosene with isopropanol or dichloromethane [54]. Years later, Suehiro *et al* used packed glass beads (200 μm diameter) and stainless steel electrodes to implement a very high throughput device (60 ml/h at cell concentration of 10^6 cells/ml) to first separate and then recover biological cells in water [55].

Chambers and channels to contain the beads and metal plates can be fabricated using standard milling techniques, injection molding or other inexpensive techniques since the dimensions required are in or above the millimeter range. Other advantages include particle filling using a

commercial dispenser, a wide variety of glass bead sizes available from many suppliers and the fact that the device can be sealed using glue or adhesive film. Since the sample is not in contact at all with the electrodes, inexpensive metals, such as aluminum which is also easy to machine, can be used to implement electrodes. Therefore, the implementation of a selective filter using this technique is relatively cheap, straight forward and features very high throughput. These characteristics make this approach a quite promising solution to implementing commercial DEP-based filters. The disadvantage is that no more advanced functions than a filter, such as focusing and particle analysis, are likely to be possible. Packing may also not be 100% reproducible leading to changes in performance during filtering. Although the electric field distribution can be inferred [56] by knowing the packing density of the beads in the channel, DEP traps cannot be designed *a priori* as it is the case when fabricating insulating structures inside the channel.

6.2 Insulator structures

The main difference between this approach and the insulator matrices described above is the fabrication of specific structures at specific places inside the microfluidic network. Pioneering work by Chou *et al* in 2002 [57] and Cummings and Singh in 2003 [58] led to the development of insulator-based devices featuring volumetric glass microstructures inside the channel. The polarizing macro electrodes can be positioned outside the channel, at its sides, or dipped in the channel at its inlet and outlet. This last approach has the advantage that the electric field can also be used to establish an electroosmotic flow inside the channel, thus gaining independence from external equipment to induce flow such as syringe pumps. However, electroosmotic flow may not be the ideal solution when targeting high throughput systems since it is a surface effect and high flow rates may not be easily achievable. Glass etching has been the most popular technique to fabricate iDEP devices but the focus is shifting towards techniques which are less expensive and less time demanding such as injection molding, casting and embossing. The work performed to this date using iDEP is significant and rapidly growing [59, 60]. Separation of many bioparticles including bacteria, cells, DNA and other biomolecules has been demonstrated. Several different geometries have been tried including single obstacle, multiple obstacles, curvature, and serpentine as shown in Figure 5. Some interesting variants of iDEP include an array of insulator structures of varying dimensions to establish insulator-gradient DEP [61], the use of serpentine-shaped channels for particle focusing [62], curved channels for particle separation [63] and the use of oil to achieve a reconfigurable insulating structure at the walls of the main channel [64]. In

this last case, oil is contained in channels perpendicular to the main channel and the protrusion of the oil meniscus into the main channel is controlled via pressure. The very recent reviews by Srivastava *et al* [59] and Regtmeier and colleagues [60] in 2011 depict well the state of the art of the technology in terms of theory, technology and applications. Therefore, further review is considered unnecessary at this moment. However, the main fabrication techniques, and the advantages and disadvantages of using each of them according to this author, are presented next to put it in context with the other techniques.

6.2.1 Glass-based structures

Insulator structures are most commonly fabricated in glass using wet etching techniques. The isotropic nature of glass etching, that is equal etching rate in all directions, severely restricts iDEP designs since gaps with aspect ratios greater than 0.5 are not possible. For example, an initial line in the etching mask of 10 μm leads to a gap of 200 μm if a channel height of 100 μm is desired. Due to this reason, most iDEP devices feature channel heights below 20 μm such that small gaps can be fabricated. Although the etch rate of glass is in the proximity of 7 $\mu\text{m}/\text{min}$ when using concentrated HF, the etching time of intricate small structures may take longer due to the hydrodynamics at play since the etchant solution must go through small openings in the mask. Glass etching process also requires an etch mask. Polymer masks, such as those in SU-8, can be used, but metal masks are preferred to minimize the possibility that pin holes in the mask negatively affect the final product. Metal masks are fabricated on the glass following a standard process of metal deposition and subsequent lift-off or wet/dry etching using a polymer mask (as detailed in section 4.1). Therefore, the fabrication of glass structures requires one more step, glass etching, than the fabrication of planar metal electrodes. Due to the isotropic etching of glass, the features in the metal mask must be smaller than the gaps required between glass structures, especially if tall structures are required. The big advantage of this technique comes in the fact that both insulator structures and the microfluidics network are simultaneously fabricated, and perfectly aligned, during glass etching. This is in contrast to other DEP techniques, including metal-electrode DEP, where the fabrication of microfluidics requires additional steps; for example, fabrication of a PDMS piece to later be aligned to the electrodes. The fabrication process of glass-based devices ends using anodic bonding to seal the etched glass to another piece of glass. A big experimental advantage of glass-based devices is that glass is a well characterized surface which is also inert and transparent. Given the surface charging of

glass, electroosmotic flow (EOF) can be readily implemented thus gaining independence from external infrastructure to establish flow such as syringe pumps. Although the electrodes used to create the electric field in iDEP can be of any conductor, (expensive) platinum wires are preferred due to their biocompatibility and because EOF and DEP can be simultaneously established by inserting these wires at the inlet and outlet of the channel. Contact between sample and electrode wires at these regions still causes electrolysis due to the DC nature of the field but the advantage is that in this case electrolysis occurs remote from the DEP active area. Although it has commonly been accepted that this electrolysis reaction does not affect DEP phenomena, the work by Gencoglu and colleagues proves that this may not be the case in all applications [65]. Products of electrolysis reactions were shown to negatively impact the observed DEP responses of biomolecules by creating a pH gradient which influences the net charge of a protein or causes aggregation during experiments.

6.2.2 Polymer-based structures

A practical disadvantage of glass-based devices is their fragility and proneness to crack, chip and break. Replacing the glass with polymers is quite beneficial [66, 67]. The cost of fabrication can be dramatically reduced since low cost batch fabrication techniques can be used such as injection molding or embossing. The main drawback of these techniques is the fabrication cost of the master mold but such expense can be easily justified in mass production operations. The choice of polymers is very wide. Resultant devices are very robust and can be disposable. Surface coatings may be needed to render the polymer biocompatible or to implement EOF but their use is highly dependent on the targeted application [68]. For example, EOF can be easily replaced by pressure-based flow, especially for high throughput systems. On the negative side, the width of the gap between structures that is achievable with injection molding and/or embossing increases proportional to the height of the features. Molding of micro-sized structures is significantly more complicated than their macro-sized counterparts [69, 70]. High aspect ratio structures, gaps or pillars, are difficult to mold or stamp due to mechanical reasons. For instance, filling of deep narrow trenches is limited by Hagen-Poiseuille flow, sharp corners are difficult to fill and high aspect ratio structures can easily break during de-molding. Furthermore, the molds used in these techniques tend to be expensive and, as in the case of stencil technology used for metal deposition, their cost is only justified if fabricating several pieces which may not always be the case in research. In any case, the push to develop injection molding and embossing for micro-

scale fabrication comes from many fields and these problems are likely to be solved in the future. The problems related to micro-molding are however not an impediment to other iDEP techniques such as curvature-induced DEP [62, 63]. In this case, micro-structures in the channel are not needed but instead curvatures in a millimeter-sized channel are exploited to create field gradients and manipulate particles. An alternative to molding and embossing is the use of micro-machining as recently demonstrated by Braff and colleagues [71]. The technique refers to the selective removal of material from a bulk using micro-sized tools. It is important to note that mechanical micro-machining is the favored technique when fabricating master molds for injection or embossing since it can provide with resolution down to 50 μm but is currently not feasible for large scale, inexpensive and rapid fabrication. Using a Microlution 363-S micro-milling machine, Braff *et al* were able to machine constrictions, with cross section of 50 by 50 μm , inside a PMMA channel. In the case of the 50 μm -high channel the constriction spans the whole height of the channel while in the case of the 500 μm -high channel the constriction is only at the top of the channel. The difference in dimension in the latter case allows the authors to implement low voltage iDEP traps which were demonstrated with latex (using 10 V) and bacterial (using 50 V) particles. The big experimental advantage of this fabrication approach is that it eliminates the need for a high voltage power supply and could reduce the impact of Joule heating during experiments. The down side is the cost and/or fragility of the infrastructure needed for fabrication. High-end micro milling machines can easily reach hundreds of thousands dollars although lower cost machines (few thousands) may also be used for certain applications. Micro-sized mill bits tend to be expensive (>100 USD a piece) and extremely fragile. Vibration, misalignment and material clogging during machining are known to cause breakage of the bit [72, 73]; incorrect handling of the tiny bits also leads to the same outcome.

A further alternative to fabricate polymer-based iDEP devices is the use of planar metal electrodes, as in metal-electrode DEP, and polymer structures fabricated with photolithography. Patterning of the metal layer is not always necessary thus reducing fabrication costs and complexity. However, metal or ITO deposition equipment is still required unless already coated substrates can be obtained elsewhere. A good example is the work from Cho and colleagues [74]. They first deposited a layer of ITO on a couple of polycarbonate (PC) pieces. In a separate process, they photo-patterned a thick SU-8 layer on top of a sacrificial layer. After dissolving the sacrificial layer, a free-standing SU-8 thick film with multiple pores in it is obtained. This

porous membrane is then positioned in between the ITO-coated PC pieces using polymer spacers in between them three to create a chamber (Figure 6). The inlet and outlet of the chamber are drilled through the PC pieces such that the sample flows from inlet to outlet going through the SU-8 membrane. During experiments, an AC voltage is applied between the ITO layers to create a uniform electric field in between them. The presence of the SU-8 membrane distorts this field with gradients created at the edges of the pores which allows for the selective trapping of bacteria. The authors claim that holes, as in their membrane, lead to higher trapping throughput than when using pillars. Other similar approaches include those by Jen and Chen, although in their case metal patterning is required [75].

6.3 Contactless DEP (cDEP)

As its name implies the main objective in this technology is to eliminate any contact between the electrode and the sample. This technique is the most recent variant to insulator-based DEP technology. While in traditional iDEP the macro electrodes are usually still in contact, although minimal, with the sample, here contact is completely eliminated as when packing glass beads inside a channel and positioning the electrodes outside the channel. Furthermore, the electrodes used here to create a DEP-active area are not solid but instead are made out of a conductive fluid. The idea is to simplify the fabrication process to only the making of a single microfluidics chip and then selectively fill some channels with a conductive liquid to use them as electrodes. A typical device contains three channels: one main channel to contain the sample and two side channels, not necessarily parallel to the main channel, on each side to contain the conductive fluid [76]. The main channel is separated at specific locations from its side channels by a polymer membrane as thin as 20 μm as shown in Figure 7. Since the polymer membrane can span the whole height of the main channel, the technique is truly 3D. These insulating barriers allow for capacitive coupling between the side channels containing the conductive fluid and the main channel. The application of an AC electric field to the conductive liquid therefore induces an electric field in the channel. Macro electrodes, usually wires, are dipped in the conductive fluid to apply the polarizing voltage. Non-uniformity of the electric field distribution inside the main channel is mainly provided by the interfaces between this channel and the meandering side channels; but can also be introduced by the presence of insulating structures. Fabrication methods are mainly based on PDMS casting using a master mold. A silicon master mold is currently first fabricated using a polymer mask and deep Reactive Ion Etching (DRIE) to achieve

etching depths up to 100 μm . The scalloping effect typical to DRIE is ameliorated by growing silicon oxide on the silicon master. The master mold is then coated with an anti-stiction layer, such as Teflon[®], before using it for casting PDMS. PDMS, in a ratio 10:1, is casted into a block containing the three channels detailed above and the separating membranes. The PDMS part is finally bonded to glass slides using oxygen plasma and interfaced fluidically using blunt needles. The side channels are then filled with conductive liquid. Phosphate buffered saline or PBS, with conductivity 1.4 S/m, is normally used given its wide availability. The technique has been used for cell sorting [77-79] and mixing [80].

The absence of contact between electrodes and the sample fluid inside the channel effectively prevents bubble formation and mitigates device fouling. Without direct contact between the electrodes and the sample fluid, any contaminating effects of this interaction can also be avoided. Voltages close to 100 V are still required to polarize the device but the voltage requirements are less than those in traditional iDEP. As with all other approaches using electrodes on the walls, an increase on channel width can have detrimental effects since DEP force decreases as one move away from the electrode surface. However, several parallel small channels each with electrodes on their walls can be implemented to increase throughput. Perhaps the main challenge is the fabrication of a robust membrane between the main channel and the side channels. The surface area of the membrane must be optimal to guarantee the membrane does not break during demolding, bonding to the glass substrate and during experiments due to pressure changes. Very thin membranes are not recommended since they are more prone to dielectric breakdown during experiments. On the other hand, as the thickness of the membrane increases higher voltage levels than those used with thinner membranes are expected to be needed to implement a similar DEP force. Therefore, the membrane must be optimized in terms of thickness and surface area to achieve both a mechanical and electrically robust membrane. One of the main advantages of this technique is that once a master mold is fabricated, the fabrication cost and complexity of experimental devices are very low. This is highly beneficial at a production stage but it can be a drawback during research and optimization as a new design with a slight change still requires a new mold. An alternative to silicon molds, where both the material and the fabrication process of the mold is less expensive would be highly beneficial. The big advantage of cDEP in terms of fabrication is that the process to make a new experimental device is reduced to one single step: casting, which is relatively easy to perform and does not require any expensive infrastructure.

The use of liquid-filled channels as microelectrodes instead of actually patterning solid materials significantly reduces the complexity of the process: electrodes in cDEP can be easily implemented by just pipetting conductive liquid into the side channels. Moreover, the conductivity of the electrode can be easily tailored by diluting a concentrated solution. As in the case of traditional iDEP, metal micro electrodes are not needed in cDEP, only metal wires to polarize the conductive fluid. But in contrast to iDEP, cDEP does not require the use of expensive platinum wire since the electrode is not at all in contact with the sample.

7. “Liquid electrode” DEP

This technique also uses metal patterning and polymer photolithography to create virtual electrodes on the channel walls. The term “liquid electrode” refers to the creation of a vertical equipotential surface at the side-walls of a channel [81]. Such surfaces can be created when fabricating narrow side channels which are perpendicular to the main channel and feature a metal electrode in its far end. The electric field generated by the planar metal electrode is guided along the narrow channel to the junction with the main channel. Therefore, the interface between the side and main channels behave as vertical “liquid electrodes” which inject the current remotely generated at the electrodes into the main channel. The concept is illustrated in Figure 8. Note that electrodes in adjacent side channels are polarized by inverted signals to generate the lateral DEP force necessary for manipulation of particles in the main channel. By adding metal electrodes, and side channels, to the other wall of the main channel a competition between the DEP forces from both sides can be used to focus and control the position of a stream of particles. Such approach is very advantageous to implement continuous particle sorting since the particle can be easily and selectively deflected to different exit channels. The fabrication process involves both metal and polymer patterning. Planar metal electrodes, around 200 nm-thick, are first fabricated on a glass substrate using metal deposition and etching or lift-off techniques. SU-8, a negative photoresist, and photolithography are then used to pattern the main and the side channels. Each side channel is patterned right on top of an individual metal pad such that only the metal edge is contained in the end of the channel. The height of the channels is usually less than 50 μm . The microfluidic network is completed by bonding a PDMS lid on top of the SU-8 channels. The PDMS lid features holes to interface connectors such as tubing or blunt needles. Such holes can be either fabricated at the time of molding or can be punched afterwards. Substantial work has

been performed using this approach and include the continuous sorting of particles [82-84], yeast cells [85] and infected blood cells [86].

The biggest advantage of this technique, as in the case of lateral flow DEP implemented with 3D metal electrodes (section 4.2), is that continuous sorting of different cell populations can be easily implemented when polarizing the electrode arrays on both sides of the channel with multiple frequencies. In the case of liquid-electrode DEP, such frequency scheme has allowed for the sorting of viable from non viable yeast cells with nearly 100% purity and a 7X enrichment of a red blood cell population infected with a parasite to obtain up to 50% infection rate in the enriched sample [83]. However, high throughput has so far not been demonstrated. The microfluidic network still features relatively low cross section thus restricting the number of cells that can be processed per unit of time. Increasing the height of the channel is unlikely to yield any benefit as long as planar electrodes are used. Increasing the width may also be detrimental since the field gradient is generated on the walls of the channel, and not on the bottom of it. The advantage of this technique over metal-electrode DEP is that large metal electrodes with gaps in the order of tens of micrometers are used. Independence from small gaps makes the fabrication process easier. The use of large electrodes also enables higher current densities and a longer electrode lifetime. The large size implies a large interfacial capacitance, and lower impedance, extending the range of operation frequencies to lower frequencies. The microfluidics network, fabricated in SU-8, does not feature small gaps either and thus the photopatterning process is relatively straight forward. A further advantage of these devices is that their operation voltage is usually lower than 30 V. The authors have reported problems when priming the channel with buffer, prior to introducing the sample. The cause is attributed to the hydrodynamics generating at the sharp corners at the interface between the side and the main channels. Particles have also been reported to get into the side channels and get physically trapped if the flow velocity is too slow.

In terms of fabrication, the merit of this approach is minimal because, although the patterns are relatively large, metal patterning and all its related processes and infrastructure are still needed. Therefore, the fabrication cost is only minimally decreased when compared to 2D metal-electrode DEP.

8. Light-induced DEP (LIDEP) and Optoelectronic Tweezers (OET)

The use of light for DEP particle manipulation has been demonstrated in many different applications including continuous particle sorting and counting [87], manipulation of DNA [88] and cells such as oocytes [89] and sperm [90], cell lysis [91], AC electroosmosis [92], separation of nanowires [93] and assembly of colloidal crystals [94] and nanoparticles [95]. A concise review on the working principle, fabrication and applications of OET is that by Jamshidi *et al* [96]. These techniques use light to excite a photoconductive layer and create an electric field gradient in the sample. The sample is contained in between a conductive layer and a photoconductive one; the photoconductive layer is on top of another conductive layer as shown in Figure 9. An AC signal is connected between the two conductive layers. It is important to note that in principle these layers are featureless and are deposited on a substrate transparent to the wavelength of the light used. When a projected light illuminates the photoconductive layer, virtual electrodes are turned on and gradients of electric field are formed. The reason for this stems from the fact that in the absence of light the impedance of the photoconductive layer is higher than the impedance of the sample and thus voltage drops mainly across the photoconductive layer; upon illumination, electron-hole pair carriers are generated in the photoconductive material thus decreasing its impedance, establishing a conductive path between the two conductive layers and causing the voltage to now drop across the sample [97]. Since light is shined in patterns and not on the whole layer the electric field in the sample becomes non-uniform. The photoconductive layer is commonly implemented using hydrogenated amorphous silicon, or a-Si:H. Amorphous silicon is the non-crystalline allotropic form of silicon. It can be deposited over large areas using PECVD (plasma-enhanced chemical vapor deposition) at temperatures as low as 75 °C which enables its deposition on plastics. Amorphous silicon is passivated by hydrogen to minimize its amount of defects and render it usable for devices. Since the whole process is conducted at low temperatures and no features are patterned in the layer, it is amenable for low cost manufacturing. However, devices fabricated this way can only work with sample conductivities smaller than 100 mS/m as reported by the pioneer authors [98]. This limitation is due to the fact that the photoconductivity of the hydrogenated amorphous silicon does not permit effective switching of the AC voltage from the photoconductive layer to the liquid layer. Although the stacking of several layers of a-Si:H increases efficiency, the use of an N+PN phototransistor structure, which features 2 orders of magnitude larger photoconductivity

than amorphous silicon, was introduced to enable the manipulation of cells in physiological media such as PBS (phosphate buffered saline) and DMEM (Dulbecco's Modified Eagle's Medium) [98]. Unfortunately, the use of this novel layer demands a more complex fabrication process. Briefly, the N+PN profile is created by two ion implantations in a highly N-doped epitaxial silicon layer. Boron (P) is implanted first followed by a drive-in step at 1000 °C for 90 minutes. Arsenic (N) is then implanted and annealed at 900 °C for 15 min. Individual pixels, with roughly the size of the cells to be manipulated when possible, are then defined and physically isolated using reactive ion etching (RIE). Finally, the pixels are electrically isolated by filling the trenches fabricated by RIE with photoresist, silicon oxide or other dielectric [98].

Different light sources are used in LIDEP and include light emitting diodes and lasers with wavelength in the 600 nm-range. The pattern shone on the photoconductive layer is usually generated using either a digital light processor (DLP®) featuring a DMD (digital micromirror device), a software mask or a Liquid Crystal Display (LCD) [99]. A microscope objective, usually 10X, is added in the optical path right before the photoconductive layer to reduce and focus the spot light. In the case of the DMD and when using the 10X microscope objective, the pixel can be as small as 1.52 μm [97].

Besides both negative and positive DEP, AC electroosmosis and electro-thermal flow have been demonstrated using these devices. The regime the device performs under depends on a combination of the polarizing frequency of the conductive layers and the optical power of the illumination light. AC Electroosmosis is mainly obtained at low frequencies regardless of the optical power. DEP is achieved at higher frequencies and low optical power while electro-thermal is obtained at a wide range of frequencies as long as the optical power remains high [100].

Watching this technique at work is something special. Different light patterns can be used to implement a variety of functions. A line can be swept along the manipulation area to selectively drag particles around, a ring can be made smaller or bigger for the same purpose. The possibilities are endless since any electrode pattern, given by the illuminating light, can be implemented. The photoconductive layer is a canvas on which one can “paint” electrodes at will. The fabrication process of these devices, in the case where the conductive and photoconductive layers are not patterned, is quite straightforward since only layer deposition is needed; no photolithography or etching. The fabrication infrastructure needed in this case is minimal

although it can be expensive. Wide surfaces can be coated with the appropriate layers and latter diced to specific size depending on the application. ITO-coated substrates can also be easily purchased from a variety of vendors. The potential for mass fabrication is high. However, ITO is relatively expensive and disposable devices may not be as feasible. The significant cost when using this technique is on the optical and illumination systems needed to create the virtual electrodes. The spot size, $\sim 1.5 \mu\text{m}$, one can achieve using a micromirror array and basic optics allows for the fabrication of quite small virtual electrodes and narrow gaps in between them which can be quite useful when manipulation nanometer-sized particles. The throughput of the device may not be high since the virtual electrodes generated using this technique are still a surface effect. Furthermore, the field of view of the optical system which in this case represents the area for particle manipulation is limited in size to a couple of centimeters square. On the other hand, the illumination system could be mounted on a motorized platform to enable wider coverage and the quick addressing of any area of the device. Implementing electrodes on the ceiling or walls of the channel represent the addition of more optical and illumination systems rendering the system complex and quite expensive. The technique is perfectly suited for single cell manipulation due to the high degree of control one has over targeted cells and the endless list of trajectories one can implement. To the best of the author's knowledge no complex microfluidics have been coupled to this kind of platform.

9. Carbon-electrode DEP (carbonDEP)

CarbonDEP combines some of the advantages of metal-based and insulator-based DEP. For example, the possibility of sample electrolysis is reduced with the use of carbon electrodes, an advantage shared with iDEP, while low voltages are enough to polarize the carbon electrodes and create an electrical field suitable for DEP, an advantage shared with metal-electrode DEP. The possibility of sample electrolysis is minimized when using carbon electrodes because carbon has a much wider electrochemical stability window than metals commonly used in thin film electrode fabrication such as gold and platinum and affords higher applied voltages in a given solution without electrolyzing it [101]. In fact, glass-like carbon is a preferred material among electrochemists [102]. Even though the electrical conductivity of glass-like carbon is lower than that of metals, suitable electric fields for DEP can be generated by polarizing carbon electrodes with voltages in the range of tens of volts instead of the hundreds or thousands of volts between

metal plates required in iDEP. The use of carbon electrodes yields other advantages: 1) excellent biocompatibility [103], 2) chemically very inert in almost all solvents/electrolytes and 3) excellent mechanical properties. Separation of latex particles, yeast and bacterial cells has been reported using these devices [18, 104, 105].

In this technique, carbon electrodes are fabricated by pyrolyzing a previously patterned organic precursor [101]. Pyrolysis refers to heating at high temperatures, up to 2000 °C but most usually to 900 °C, in inert atmosphere such as nitrogen, forming gas or vacuum. During pyrolysis, all materials other than carbon are eliminated from the matrix and one ends up with glass-like carbon, a material commonly known as glassy carbon due to its wide commercialization under such name. The organic precursor of the carbon electrodes used for DEP applications has usually been photoresists such as SU-8 or AZ, a positive-tone one, but in principle many other precursors could be used. Photolithography is commonly used to pattern the organic precursor given the small dimensions one can achieve with such technology. Other low cost techniques can also be used such as embossing and molding. 3D carbon structures can be relatively easy to fabricate since polymer patterning is the only process needed. In a typical process (shown in Figure 10), a SU-8 precursor is patterned in two steps, the first a planar layer to fabricate what will be the pads and connection leads to the base of the volumetric electrodes; and a second step to fabricate the volumetric structures that will become the 3D carbon electrodes. The photopatterned polymer is then carbonized by following a heating ramp of 5-10 °C/min to 900 °C and dwelling at this temperature for one hour. The samples are then let to cool naturally. Carbon electrodes as high as 100 µm are routinely used in this technique [104] but electrodes with height up to 273 µm have been demonstrated [106]. The electrical resistivity of the resultant glass-like carbon is around $1 \times 10^{-4} \Omega \cdot \text{m}$ [106, 107]. This value is in the same order of magnitude of indium tin oxide but four orders of magnitude higher than that of gold. The type of substrate for fabrication is highly important since not many materials maintain integrity at very high temperatures. Those that do are usually more expensive than the common float glass used in metal patterning or insulator-based DEP. Common substrates are opaque silicon, with or without silicon oxide coating, and fused silica [104]. The polymer precursor structures shrink during carbonization and therefore one must take this into account when designing the electrodes. The shrinkage varies depending on the original dimensions of the polymer structure but is highly reproducible given a precursor type. For example, shrinkage up to 90% in height can be present

when carbonizing SU-8 structures as thick as 10 μm but the shrinkage decreases to 30% when pyrolyzing structures with thickness greater than 300 μm . Shrinkage of a polymer structure attached to a substrate of different material, in this case SU-8 on fused silica or silicon, is not isometric. Further details regarding the carbonization of short and tall SU-8 structures can be found in the works by Park *et al* [107] and Martinez-Duarte *et al* [104] respectively. The microfluidics network is fabricated separate from the carbon electrodes and later aligned to the electrode array. The network is made by stacking drilled polycarbonate pieces and double-sided adhesive [104]. The polycarbonate piece becomes the ceiling of the device and features the channel inlet and outlet. The micro-sized channels are cut into the adhesive using a standard cutter plotter. The height of the channel is given by the thickness of the adhesive. Different thicknesses values, and as thin as 25 μm , are commercially available. After aligning the microfluidics network to the carbon electrode array, the device is closed and sealed using a cold laminator. This approach leads to very robust devices capable of handling high pressures without any leaking. For example, based on the experience of this author flow rates up to few ml/min can be implemented in a channel cross-section of 100 μm by 2 mm without leakage.

The fabrication of carbon electrodes is relatively simple and inexpensive as it only requires polymer photolithography and heat treatment. A pyrolysis furnace can cost a few tens of thousands dollars. No metal processing, *i.e.* sputtering, evaporation or electroplating, is required. Shrinkage during pyrolysis is observed to be dependent on the dimensions of the initial SU-8 structure and can be an important obstacle when narrow gaps between tall electrodes are desired. A potential disadvantage of carbonDEP is the electrical resistivity of glass-like carbon, which is four and three orders of magnitude more than that of gold and platinum respectively. The voltage loss that develops from the ohmic resistance in the narrow leads connecting the base of the electrodes and the function generator makes it necessary to use higher voltage levels than those used in metal-electrode DEP. A voltage below 20 V_{pp} has been demonstrated to be sufficient to create a suitable DEP force to manipulate eukaryotic cells when using carbon electrodes and thus there is no need for an additional signal amplifier. The real need for metal connecting leads from the function generator to the base of the 3D electrodes must be assessed depending on the application. For example, the need for gaps between 3D electrodes $<20 \mu\text{m}$ would require the connecting leads to be quite narrow. At such dimensions, the ohmic resistance of carbon leads can require the use of hundreds of volts and the use of metal leads can be highly beneficial. A big

advantage of this technique is on material cost since metals, especially precious ones, are significantly more expensive than polymers used as carbon precursors. While metal and glass etching require sacrificial layers of polymers during processing; carbon fabrication only requires the carbonization of polymers. Therefore, the fabrication process is simplified and less expensive while the cost of the materials involved is relatively low. A disadvantage of carbonDEP is the cost of the substrate, especially when compared to the cost of float glass substrates commonly used in metal-electrode DEP or the cost of polymers used in iDEP. However, the potential of the technique to fabricate inexpensive tall 3D structures may overcome this disadvantage. Many carbon electrodes may be first fabricated on a silicon or fused silica wafer, the wafer then diced into smaller pieces (which will become a DEP-active area) and these pieces finally packaged in cheaper materials to obtain an experimental device. This approach, similar to the one used in the integrated-circuit industry, can greatly minimize the cost of each device.

10. Metal injection and co-fabrication

Co-fabrication is a strategy for fabricating multiple structures in a single step by injecting functional materials into pre-fabricated cavities [108]. It generates correct alignment in micro components in a fast and inexpensive way since material injection is the only step needed, provided the structure containing the cavities to be filled is already available. This approach was already touched upon in the case of contactless DEP where the side channels are filled with a conductive liquid. Most recently, So and Dickey used co-fabrication to fabricate a DEP device featuring a main channel with metal electrodes on its walls [109]. The fabrication process starts by making a PDMS part using soft lithography and SU-8 mold. The PDMS part is then bonded to a glass slide or another PDMS part producing simultaneously the fluidic channel and the electrode channels. A liquid metal is injected in the electrode channels by hand using a syringe. They focus on the use of eutectic gallium indium (EGaIn, Ga 75%, In 25% by weight) because its low viscosity at room temperature (approximately twice as thick as water) allows injection by hand. However, they also demonstrated injection of molten metals such as Gallium (melting point 30 °C) and indium alloy (InBiSn, In 51%, Bi 32.5% and Sn 16.5 % by weight, melting point 60 °C). These two later materials are advantageous since they are solids at room temperature and thus their shape is easier to control than liquids. The flow of the liquid-phase metal once inside the electrode channel can be controlled by a variety of geometries. For

example, the authors used a line of posts separating the main channel from the electrode channel to implement capillary valves which prevent the liquid metal from entering the main channel. Since the distance between two neighboring posts ($50\ \mu\text{m}$) is much smaller than the width of the electrode channels ($1000\ \mu\text{m}$), but yet have the same height, the pressure required to inject the metal through the electrode channels is almost half of that required to inject it between the posts. In such a way they fabricated long metal electrode walls along the channel with perfect alignment. Other geometries include the use of electrode channels perpendicular to the main channel such that upon injection metal electrodes protrude into the main channel. It is important to note that the electrodes can be exactly equal to the height of the channel. Such alignment perfection would be challenging to fabricate with conventional deposition process.

The advantages of this approach are similar to those of cDEP in that the fabrication process is a single-step casting. However, in this case no thin membranes are required and thus the fabrication constraints are relaxed (but the disadvantage of having the metal in contact with the sample arises). The casting mold used in the approach just detailed is made by standard photolithography which is significantly less expensive than DRIE currently used for cDEP. As with cDEP, the use of co-fabrication is highly beneficial because it allows for rapid functionalization of the device by introducing a liquid metal, conductive liquid or molten metal in specific channels. The creation of an experimental setup is thus fairly quick once a mold is available. The disadvantages of using metal in contact with the sample have been detailed before and also apply in this case. In particular, the use of liquid-phase EGaIn represents a challenge to the robustness of the device since the liquid metal shape is only stabilized by a thin oxide surface layer. Although this layer is not anticipated to be detrimental to the electrical behavior of the electrodes, the oxide skin may be dissolved via reduction when the electrode is biased. Without the oxide skin the liquid metal would flow and change its shape spontaneously to reduce its surface energy which can significantly impact experiments. A study of the stability of the oxide skin has been presented elsewhere [109]. The use of low melting point metals which solidify just after being introduced in the channels can eliminate this problem. However, heating during experiments may be strong enough to melt them causing a shape change and a different distribution of the electric field in the sample. Metals with higher melting point may also be used. In this case care must be taken to prevent any negative effect of higher temperatures on other materials in the device, especially PDMS.

11. Doped PDMS

PDMS has been mainly used to fabricate the microfluidics networks in DEP devices. Recently, it has been implanted with metal ions or loaded with conductive particles to achieve a PDMS-based conductive composite used as electrode in microfluidic applications. Niu and collaborators achieved both silver- and carbon-loaded PDMS composites [110]. After characterizing the conductivity of the composite depending on percentage loading, they found out that conductivities above 10^4 S/m can be obtained when loading above 86 wt% in the case of silver and 26 wt% in the case of carbon black. The same authors introduced the patterning and integration of these composites in microfluidics devices [111]. The fabrication process starts by patterning thick layers of AZ resist around SU-8 features previously fabricated on the substrate. The SU-8 features define the microfluidic network which will contain the sample while the AZ features the locations of the composite electrodes. The cavities around the SU-8 features, made by AZ patterning, are then filled with PDMS-based composite and excess of the composite is cleaned with a blade. After the composite is thermally cured and stable inside the AZ topography, AZ is removed leaving only SU-8 and composite topographies on the substrate. Pure PDMS is then casted on this topography, thermally cured and de-molded. Since the composite has more affinity for the pure PDMS than the SU-8 one obtains a PDMS block with embedded composite electrodes interfaced to the microfluidic network. The PDMS piece is then treated with oxygen plasma and bonded on a glass slide to obtain an experimental device as shown in Figure 11. Holes are then punched and fluidic connectors, such as tubing or blunt needles, are installed. If cleaned properly, the SU-8 mold can be used again. The use of these techniques in different microfluidics applications, including droplet detection and control [112], has been recently reviewed [111]. In regard to DEP, the use of a silver-based composite was demonstrated for cell focusing by Lewpiriyawong *et al* in 2010 [113]. Their device featured 40 μm -high SU-8 channels with electrodes on its walls. These electrodes are 100 μm wide with equal separation between them. They are connected to the function generator using alligator clips. An 85 wt% loading of silver was used to achieve conductivity of 2×10^4 S/m. The authors note that higher percentage of silver loading makes the composite too powdery to mix and place in the AZ cavities. The use of carbon black-loaded PDMS in DEP applications was demonstrated by Deman *et al* in 2011 [114]. Their fabrication technique differs slightly from that detailed before in that they replaced the AZ photoresist by dry film photoresist. The dry film pattern now defines

the cavities where the carbon-PDMS composite will be deposited around the SU-8 structures. After thermally curing the composite the dry film is dissolved with ethanol and pure PDMS is casted on the mold. The PDMS with the carbon-PDMS composite is then de-molded, plasma treated and bonded to a glass substrate. The channel is 100 μm -high with electrodes spanning its whole height. Gold tracks are previously patterned on the glass substrate using metal deposition and wet etching through a polymer mask. These tracks provide a way to connect the composite electrode to a function generator.

The fabrication process used in this technique is again based on casting. However, here the fabrication process requires more steps than only casting PDMS. The fabrication of the PDMS-based composite appears to be straight forward but a minimal level of homogeneity in mixing the filler in the matrix must be guaranteed to obtain reproducible values of the conductivity of the composite. The cost of the conductive filler, in this case carbon black and silver particles, must be added to the total cost of the device. Other than equipment to obtain the PDMS composite (balance and a mixing instrument which can be as simple as a handheld mixer), standard photolithography equipment is the only fabrication infrastructure needed. A potential disadvantage of the doped PDMS electrodes is its surface roughness since the protruding of particles out of the polymer surface can introduce local field gradients that could be strong enough to affect the cells. Although the bulk of the metal is immersed in the PDMS matrix, contact between sample and metal, although minimal, is still present. In the case of silver, this contact could be detrimental to the viability of bacteria and cells, given the known toxicity of silver to these species [115, 116].

Metal ion implantation has also been used to fabricate electrodes along the walls of a PDMS channel. Choi *et al* first fabricated a rectangular channel with cross section 100 μm -wide and 70 μm -high using PDMS casting on a SU-8 mold [117]. Low energy metal ion implantation is then used to coat the inside of the channel with gold ions through a steel shadow mask (two openings of 8 mm by 15 mm each separated by 100 μm). The implantation is conducted twice at 40° angle to create mirror image electrodes within the fluidic channel. The thickness of the electrodes is 50 nm. Based on such thickness and the measured sheet resistance of the implanted gold of 100 Ω/square , conductivity of the electrodes is assumed to be $2 \times 10^5 \text{ S/m}$. After metal implantation, gold electrodes are sputtered on the edges of the previously implanted layer to guarantee good electrical connection between the implanted layer and ITO electrodes patterned on a glass slide

(to become the bottom of the channel) as detailed next. An ITO-coated glass slide is separately patterned to both create electrical contacts to the gold implanted region and to provide electrodes for the bottom of the microfluidics channel. After punching connection holes in the gold-coated PDMS, the patterned glass slide and the PDMS piece are brought together and sealed closed using oxygen plasma. At the end, the channel features 8 different electrodes, four planar ones at the bottom made in ITO and four 3D ones on the walls and ceiling of the channel made by gold implantation as shown in Figure 12. By separately controlling each of them, great flexibility in specifying direction and distribution of the electric field is obtained as simulated by the authors.

The fabrication process used in this approach consist of PDMS casting, metal ion implantation through a shadow mask and ITO and metal patterning which requires photolithography and etching. Because all these different steps the fabrication process does not look amenable for low cost production. Although the amount of metal used to fabricate the 3D electrodes on the walls of the channel is minimal, still requires infrastructure for metal deposition. Thin metal electrodes on a flexible substrate may also be prone to crack. The device appears to be more useful to manipulate and analyze single cells, when the use of an octopole trap may yield significant advantages such as exquisite control of cell motion in all axes.

12. Overview of Microfluidics fabrication

A summary of the so far published processes and materials needed to fabricate micro-scaled DEP active-elements: electrodes, insulator structures, etc., is presented in Table 1. A basic light-induced DEP device features the simplest fabrication. Fabrication of iDEP devices based on the use of glass beads seems to be the least expensive. Remarks about the most common ways to incorporate a microfluidics network to a DEP-active element are also included. This is to provide the reader with a complete overview of the cost and complexity of all the processes needed to obtain an experimental device. The most common, and well known, means to fabricate a microfluidics network are 1) soft lithography, or the use of a mold to cast a PDMS part which is then plasma activated and sealed against a substrate; or 2) the use of photolithography to directly pattern a network on a substrate. Soft lithography is by far the most popular process. In most of the DEP techniques, PDMS casting is used to fabricate a microfluidics network that is later positioned around an electrode array. Other most recent techniques, such as contactless or metal injection-based, use PDMS parts containing a microfluidics network that both enables sample

handling and will give rise to the DEP-active areas after injection of a conductive liquid or a liquid metal. When using the doped-PDMS technique, the fluidic network is made in the pure PDMS part that is later functionalized by incorporating conductive particle or by metal ion-implantation.

Another common approach is to pattern a film of photoresist, deposited by spin-coating or by lamination of a dry film, directly on the substrate. In this way, open (without a ceiling) channels and chambers can be perfectly aligned to the electrodes on the substrate. An extra step is needed here to close the fluidics network. Common techniques to do so include a drilled plastic or glass lid and glue, *i.e.* UV or epoxy-based, double-sided adhesives or solvent-assisted bonding for plastics. A more straightforward alternative to both of these approaches, soft lithography and photolithography, is the use of a cutter plotter to pattern a film of adhesive with channels and chambers. This patterned adhesive is then stacked against a lid, which is usually drilled to provide with inlets and outlets, and such stack is directly adhered on a substrate. The device is sealed using a rolling press. Based on this author's experience with the three approaches [106], the use of patterned adhesives [18,104] allows for leak-free devices capable of handling flow rates of up to few milliliters per second in a channel cross-section as small as 100 μm -high and 1 mm-wide. Although the current resolution of a cutter plotter is in the sub-mm range, useful designs for DEP, and other applications, can be fabricated. The most significant advantage comes from the fact that this approach does not make use of a cleanroom in any way and allows the fabrication of a completely new microfluidics design on-site and within minutes. Furthermore, the infrastructure needed only costs a couple thousand US dollars and inexpensive adhesive films of many different thicknesses, and different properties, are widely available (for example from Adhesive Research and FLEXcon).

Lastly, other techniques such as glass-based insulator-based DEP and doped-silicon DEP, offer the advantage that an open microfluidics network is patterned together with the insulator structures or the electrodes. However, a significant disadvantage of these techniques is the need for anodic bonding to close the device.

13. Perspectives on the future

The main target for the coming years is to make fabrication processes of DEP devices inexpensive and simple enough while also improving their user-friendliness, throughput,

robustness and reproducibility. The goal is to accelerate the validation, and daily use, of DEP in practical settings.

As seen in Table 1, the complexity, cost and number of fabrication processes used in DEP techniques such as light-induced, carbon-electrode and contactless; is less than those in conventional techniques such as metal-electrode and traditional iDEP devices based on glass micro-structures. The current worldwide emphasis on the synthesis and applications of new materials could bring yet another boost to DEP technology. For example, the advantages, if any, of using graphene as electrode material in DEP are still to be demonstrated; conductive polymers such as Poly(3,4-ethylenedioxythiophene) poly(styrenesulfonate), commonly known as PEDOT:PSS, or polypyrrole have not been used as DEP electrodes to the best of this author's knowledge; new composites which increase the conductivity, porosity and inertness of the electrodes also show great potential. Inexpensive conductive materials featuring excellent electrochemical properties and low cost patterning processes could make disposable DEP devices and a point-of-care platform (using practical voltages) a reality. Imagine a cell sorting device which can output the blood cell composition, and presence of pathogens, in real-time at the intensive care unit or surgical table. Regarding a substrate material, if it is indeed needed, the use of transparent ones are not a must but they are preferred to facilitate the monitoring of an assay and quantify results with widely used techniques such as optical spectrometry. Plastics are here a perfect alternative to glass, given the plastic or polymer material does not interfere with an optical measurement and is chemically and biologically inert. Efforts on quantifying assay results with non-optical techniques are also important, such as the use of impedance spectrometry [118], towards simplifying an experimental platform.

Throughout the years, the supporting infrastructure for DEP chips has become more sophisticated towards offering user-friendly platforms. This point is extremely important since often DEP is regarded as a complex, fragile and unreliable technique. Simple and robust plug and play devices are desired to enable their daily use by non-technical staff. Initial efforts on this direction is the use of a PCB (printed circuit board), completely fitted with signal conditioners, as a DEP chip holder [48, 119]. In this case the user only needs three steps to set up an experimental platform: 1) insert the DEP chip in the PCB, 2) connect the function generator to the PCB and 3) plug the flow management infrastructure, a pressure pump and tubing for example, to the chip. Further efforts are on eliminating external equipment needed for flow

management while keeping the PCB approach [18]. The elimination of pumps, tubing and external fluidic interconnects (which are often expensive) effectively reduces the footprint of a DEP platform and makes it significantly cheaper, self-enclosed and less prone to leakage. In this context, the use of electroosmotic flow has proven beneficial although the flow established is highly dependent on the conditions of the channel surface. The use of centrifugal microfluidics [18] and gravity [120] has also been demonstrated to obtain portable, self-contained DEP platforms. Efforts towards also eliminating external and bulky function generators have been reported by Gomez-Quñones *et al* [121] who developed a CMOS electronic chip for synthesizing a number of functions. This electronic chip, with footprint of 1.56 by 2.03 mm, can then be mounted on a PCB together with the DEP device to obtain a stand-alone DEP platform that only needs connection to power and a user interface. Power may come from a wall outlet, batteries or a USB connection. The interface could be as simple as a desktop connection, an embedded system or remote control and data gathering using a portable device. A major milestone will be a low cost sample-to-answer system where the user only needs to insert a DEP chip into the platform, load the sample and press a button to start an assay. The answer can be a) strings of data for complete blood counts or diagnostics; or b) enriched particle populations for therapeutics or further analysis, such as PCR or proteomics. Such system could become a less expensive, label-free alternative to current flow cytometry and magnet-based instruments.

As a conclusion, the fabrication process of DEP devices and its supporting infrastructure has advanced significantly in the last 20 years and, as more applications are demonstrated, the quest for an ideal technology is as active as ever. The state-of-the-art of microfabricating DEP devices has been critically reviewed in this work in terms of complexity, cost and throughput. Given that the throughput of DEP devices has been steadily increasing and the cost and complexity of the fabrication techniques is constantly decreasing, this author is confident DEP will become an important technique in settings other than research in the coming years. There is however still plenty of room for improvement, so let us keep working.

Declaration of Conflict of Interest: Rodrigo Martinez-Duarte is one of the main authors behind DEP technology using carbon electrodes. The interest is not financial.

References

- [1] Pohl, H. A., *J Appl Phys* 1951, 22, 869.
- [2] Pethig, R., *Biomicrofluidics* 2010, 4, 022811.
- [3] Gascoyne, P. R. C., Vykoukal, J. V., *P IEEE* 2004, 92, 22-42.
- [4] Jesús-Pérez, N. M., Lapizco-Encinas, B. H., *Electrophoresis* 2011, 32, 2331-2357.
- [5] Krupke, R., *Science* 2003, 301, 344-347.
- [6] Raychaudhuri, S., Dayeh, S. A., Wang, D., Yu, E. T., *Nano Lett* 2009, 9, 2260-2266.
- [7] Tang, J., Yang, G., Zhang, Q., Parhat, A., Maynor, B., Liu, J., Qin, L.-C., Zhou, O., *Nano Lett* 2005, 5, 11-14.
- [8] Kalantar-zadeh, K., Khoshmanesh, K., Kayani, A. A., Nahavandi, S., Mitchell, A., *Appl Phys Lett* 2010, 96, 101108.
- [9] Hölzel, R., Calander, N., Chiragwandi, Z., Willander, M., Bier, F., *Phys Rev Lett* 2005, 95.
- [10] Fuhr, G., Schnelle, T., Muller, T., Hitzler, H., Monajembashi, S., Greulich, K.-O., *Appl Phys A-Mater* 1998, 67, 385-390.
- [11] Graham, D. M., Messerli, M. A., Pethig, R., *Biotechniques* 2012, 52, 39-43.
- [12] Gagnon, Z. R., *Electrophoresis* 2011, 32, 2466-2487.
- [13] Lapizco-Encinas, B. H., Rito-Palomares, M., *Electrophoresis* 2007, 28, 4521-4538.
- [14] Holzel, R., *IET Bionanotechnol* 2009, 3, 28-45.
- [15] Meighan, M. M., Staton, S. J. R., Hayes, M. A., *Electrophoresis* 2009, 30, 852-865.
- [16] Hughes, M. P., *Electrophoresis* 2002, 23, 2569-2582.
- [17] Markx, G. H., *Organogenesis* 2008, 4, 11-17.
- [18] Martinez-Duarte, R., Gorkin Iii, R. A., Abi-Samra, K., Madou, M. J., *Lab Chip* 2010, 10, 1030.
- [19] Pohl, H. A., *J Appl Phys* 1958, 29, 1182.
- [20] Pohl, H. A., Schwar, J. P., *J Appl Phys* 1959, 30, 69.
- [21] Pohl, H. A., Plymale, C. E., *J Electrochem Soc* 1960, 107, 390-396.
- [22] Pohl, H. A., Schwar, J. P., *J Electrochem Soc* 1960, 107, 383-385.
- [23] Pohl, H. A., Hawk, I., *Science* 1966, 152, 647-649.
- [24] Pohl, H. A., Crane, J. S., *Biophys J* 1971, 11, 711-727.

- [25] Ting, I. P., Jolley, K., Beasley, C. A., Pohl, H. A., *Biochim Biophys Acta* 1971, 234, 324-329.
- [26] Pohl, H. A., *J Biol Phys* 1973, 1, 1-16.
- [27] Chen, C. S., Pohl, H. A., *Ann NY Acad Sci* 1974, 238, 176-185.
- [28] Rhoads, J. E., Pohl, H. A., *J Biol Phys* 1976, 4, 93-108.
- [29] Pohl, H. A., Pollock, K., *J Electrostat* 1978, 5, 337-342.
- [30] Pohl, H. A., *J Biol Phys* 1979, 7, 1-16.
- [31] Kaler, K., Pohl, H. A., *IEEE T Ind Appl* 1983, 19, 1089-1093.
- [32] Price, J. A. R., Burt, J. P. H., Pethig, R., *Biochim Biophys Acta* 1988, 964, 221-230.
- [33] Vazquez-Mena, O., Villanueva, G., Savu, V., Sidler, K., van den Boogaart, M. A. F., Brugger, J., *Nano Lett* 2008, 8, 3675-3682.
- [34] Manaresi, N., Romani, A., Medoro, G., Altomare, L., Leonardi, A., Tartagni, M., Guerrieri, R., *IEEE J Solid-St Circ* 2003, 38, 2297-2305.
- [35] Medoro, G., Manaresi, N., Leonardi, A., Altomare, L., Tartagni, M., Guerrieri, R., *IEEE Sens J* 2003, 3, 317-325.
- [36] Fuchs, A. B., Romani, A., Freida, D., Medoro, G., Abonnenc, M., Altomare, L., Chartier, I., Guergour, D., Villiers, C., Marche, P. N., Tartagni, M., Guerrieri, R., Chatelain, F., Manaresi, N., *Lab Chip* 2006, 6, 121.
- [37] Fiedler, S., Shirley, S., Schnelle, T., Fuhr, G., *Anal Chem* 1998, 70, 1909-1915.
- [38] Muller, T., Gradi, G., Howitz, S., Shirley, S., Schnelle, T., Fuhr, G., *Biosens Bioelectron* 1999, 14, 247-256.
- [39] Schnelle, T., Muller, T., Gradl, G., Shirley, S., Fuhr, G., *J Electrostat* 1999, 47, 121-132.
- [40] Voldman, J., Gray, M. L., Toner, M., Schmidt, M., *Anal Chem* 2002, 74, 3984-3990.
- [41] Wang, L., Flanagan, L. A., Lee, A. P., *J Microelectromech S* 2007, 16, 454-461.
- [42] Wang, L., Flanagan, L. A., Jeon, N. L., Monuki, E., Lee, A. P., *Lab Chip* 2007, 7, 1114.
- [43] Wang, L., Lu, J., Marchenko, S. A., Monuki, E. S., Flanagan, L. A., Lee, A. P., *Electrophoresis* 2009, 30, 782-791.
- [44] Fatoyinbo, H. O., Kanchis, D., Whattingham, R., Ogin, S. L., Hughes, M. P., *IEEE T Bio-Med Eng* 2005, 52, 1347-1349.
- [45] Park, B. Y., Madou, M. J., *Electrophoresis* 2005, 26, 3745-3757.
- [46] Abidin, Z. Z., Downes, L., Markx, G. H., *J Biotechnol* 2007, 130, 183-187.

- [47] Gencoglu, A., Minerick, A., *Lab Chip* 2009, 9, 1866.
- [48] Park, K., Suk, H.-J., Akin, D., Bashir, R., *Lab Chip* 2009, 9, 2224.
- [49] Iliescu, C., Xu, G. L., Samper, V., Tay, F. E. H., *J Micromech Microeng* 2005, 15, 494-500.
- [50] Yu, L., Tay, F. E. H., Xu, G. L., Iliescu, C., *Int J Softw Eng Know* 2005, 15, 231-236.
- [51] Iliescu, C., Yu, L., Xu, G., Tay, F. E. H., *J Microelectromech S* 2006, 15, 15061513.
- [52] Iliescu, C., Xu, G. L., Ong, P. L., Leck, K. J., *J Micromech Microeng* 2007, 17, S128-S136.
- [53] Lin, I. J., Benguigui, L., *J Electrostat* 1982, 13, 257-278.
- [54] Benguigui, L., Lin, I. J., *J Appl Phys* 1984, 56, 3294.
- [55] Suehiro, J., Zhou, G., Imamura, M., Hara, M., *IEEE T Ind Appl* 2003, 39, 1514-1521.
- [56] Abidin, Z. Z., Marx, G. H., *J Electrostat* 2005, 63, 823-830.
- [57] Chou, C.-F., Tegenfeldt, J. O., Bakajin, O., Chan, S. S., Cox, E. C., Darnton, N., Duke, T., Austin, R. H., *Biophys J* 2002, 83, 2170-2179.
- [58] Cummings, E. B., Singh, A. K., *Anal Chem* 2003, 75, 4724-4731.
- [59] Srivastava, S. K., Gencoglu, A., Minerick, A. R., *Anal Bioanal Chem* 2010, 399, 301-321.
- [60] Regtmeier, J., Eichhorn, R., Viefhues, M., Bogunovic, L., Anselmetti, D., *Electrophoresis* 2011, 32, 2253-2273.
- [61] Pysher, M. D., Hayes, M. A., *Anal Chem* 2007, 79, 4552-4557.
- [62] Zhu, J., Tzeng, T.-R. J., Hu, G., Xuan, X., *Microfluid Nanofluid* 2009, 7, 751-756.
- [63] Zhang, L., Tatar, F., Turmezei, P., Bastemeijer, J., Mollinger, J. R., Piciu, O., Bossche, A., *J Phys Conf Ser* 2006, 34, 527-532.
- [64] Thwar, P. K., Linderman, J. J., Burns, M. A., *Electrophoresis* 2007, 28, 4572-4581.
- [65] Gencoglu, A., Camacho-Alanis, F., Nguyen, V. T., Nakano, A., Ros, A., Minerick, A. R., *Electrophoresis* 2011, 32, 2436-2447.
- [66] McGraw, G. J., Davalos, R. V., Brazzle, J. D., Hachman, J., Hunter, M. C., Chames, J., Fiechtner, G. J., Cummings, E. B., Fintschenko, Y., Simmons, B. A., *Proc Spie* 2005, 5715, 59-68.
- [67] Simmons, B. A., McGraw, G. J., Davalos, R. V., Fiechtner, G. J., Fintschenko, Y., Cummings, E. B., *MRS Bulletin* 2006, 31, 120-124.
- [68] Davalos, R. V., McGraw, G. J., Wallow, T. I., Morales, A. M., Krafcik, K. L., Fintschenko, Y., Cummings, E. B., Simmons, B. A., *Anal Bioanal Chem* 2007, 390, 847-855.
- [69] Hecke, M., Schomburg, W. K., *J Micromech Microeng* 2004, 14, R1-R14.

- [70] Giboz, J., Copponnex, T., Mélé, P., *J Micromech Microeng* 2007, 17, R96-R109.
- [71] Braff, W. A., Pignier, A., Buie, C. R., *Lab Chip* 2012, 12, 1327-1331.
- [72] Dornfeld, D., Min, S., Takeuchi, Y., *CIRP Ann-Manuf Techn* 2006, 55, 745-768.
- [73] Cheng, X., Wang, Z., Nakamoto, K., Yamazaki, K., *Int J Adv Manuf Tech* 2010, 53, 523-533.
- [74] Cho, Y.-K., Kim, S., Lee, K., Park, C., Lee, J.-G., Ko, C., *Electrophoresis* 2009, 30, 3153-3159.
- [75] Jen, C.-P., Chen, T.-W., *Microsyst Technol* 2008, 15, 1141-1148.
- [76] Shafiee, H., Caldwell, J. L., Sano, M. B., Davalos, R. V., *Biomed Microdevices* 2009, 11, 997-1006.
- [77] Shafiee, H., Sano, M. B., Henslee, E. A., Caldwell, J. L., Davalos, R. V., *Lab Chip* 2010, 10, 438.
- [78] Henslee, E. A., Sano, M. B., Rojas, A. D., Schmelz, E. M., Davalos, R. V., *Electrophoresis* 2011, 32, 2523-2529.
- [79] Salmanzadeh, A., Romero, L., Shafiee, H., Gallo-Villanueva, R. C., Stremmler, M. A., Cramer, S. D., Davalos, R. V., *Lab Chip* 2012, 12, 182-189.
- [80] Salmanzadeh, A., Shafiee, H., Davalos, R. V., Stremmler, M. A., *Electrophoresis* 2011, 32, 2569-2578.
- [81] Demierre, N., Braschler, T., Linderholm, P., Seger, U., van Lintel, H., Renaud, P., *Lab Chip* 2007, 7, 355.
- [82] Demierre, N., Braschler, T., Muller, R., Renaud, P., *Sensor Actuat B-Chem* 2008, 132, 388-396.
- [83] Valero, A., Braschler, T., Demierre, N., Renaud, P., *Biomicrofluidics* 2010, 4, 022807.
- [84] Braschler, T., Demierre, N., Nascimento, E., Silva, T., Oliva, A. G., Renaud, P., *Lab Chip* 2008, 8, 280.
- [85] Mernier, G., Piacentini, N., Tornay, R., Buffi, N., Renaud, P., *Procedia Chemistry* 2009, 1, 385-388.
- [86] Nascimento, E. M., Nogueira, N., Silva, T., Braschler, T., Demierre, N., Renaud, P., Oliva, A. G., *Bioelectrochemistry* 2008, 73, 123-128.
- [87] Lin, Y.-H., Lee, G.-B., *Biosens Bioelectron* 2008, 24, 572-578.
- [88] Hoeb, M., Rädler, J. O., Klein, S., Stutzmann, M., Brandt, M. S., *Biophys J* 2007, 93, 1032-1038.
- [89] Hwang, H., Lee, D.-H., Choi, W., Park, J.-K., *Biomicrofluidics* 2009, 3, 014103.

- [90] Ohta, A. T., Garcia, M., Valley, J. K., Banie, L., Hsu, H.-Y., Jamshidi, A., Neale, S. L., Lue, T., Wu, M. C., *Lab Chip* 2010, *10*, 3213.
- [91] Lin, Y.-H., Lee, G.-B., *Appl Phys Lett* 2009, *94*, 033901.
- [92] Chiou, P. Y., Ohta, A. T., Jamshidi, A., Hsu, H.-y., Wu, M. C., *J Microelectromech S* 2008, *17*, 525-531.
- [93] Jamshidi, A., Pauzauskie, P. J., Schuck, P. J., Ohta, A. T., Chiou, P.-Y., Chou, J., Yang, P., Wu, M. C., *Nat Photonics* 2008, *2*, 86-89.
- [94] Hayward, R. C., Saville, D. A., Aksay, I. A., *Nature* 2000, *404*, 56-59.
- [95] Jamshidi, A., Neale, S. L., Yu, K., Pauzauskie, P. J., Schuck, P. J., Valley, J. K., Hsu, H.-y., Ohta, A. T., Wu, M. C., *Nano Lett* 2009, *9*, 2921-2925.
- [96] Jamshidi, A., Ohta, A. T., Valley, J. K., Hsu, H.-Y., Neale, S. L., Wu, M. C., *Proc Spie* 2008, *6993*, 69930A-69930A-69910.
- [97] Chiou, P. Y., Ohta, A. T., Wu, M. C., *Nature* 2005, *436*, 370-372.
- [98] Hsu, H.-y., Ohta, A. T., Chiou, P.-Y., Jamshidi, A., Neale, S. L., Wu, M. C., *Lab Chip* 2010, *10*, 165.
- [99] Choi, W., Kim, S.-H., Jang, J., Park, J.-K., *Microfluid Nanofluid* 2006, *3*, 217-225.
- [100] Valley, J. K., Jamshidi, A., Ohta, A. T., Hsu, H.-y., Wu, M. C., *J Microelectromech S* 2008, *17*, 342-350.
- [101] Wang, C., Jia, G., Taherabadi, L., Madou, M., *J Microelectromech S* 2005, *14*, 348-358.
- [102] van der Linden, W. E., Dieker, J. W., *Analytica Chimica Acta* 1980, *119*, 1-24.
- [103] Turon Teixidor, G., Gorkin, R. A., Tripathi, P. P., Bisht, G. S., Kulkarni, M., Maiti, T. K., Battacharyya, T. K., Subramaniam, J. R., Sharma, A., Park, B. Y., Madou, M., *Biomed Mater* 2008, *3*, 034116.
- [104] Martinez-Duarte, R., Renaud, P., Madou, M. J., *Electrophoresis* 2011, *32*, 2385-2392.
- [105] Jaramillo, M. d. C., Torrents, E., Martínez-Duarte, R., Madou, M. J., Juárez, A., *Electrophoresis* 2010, *31*, 2921-2928.
- [106] Martinez-Duarte, R., *Mechanical and Aerospace Engineering*, Ph. D. University of California, Irvine, 2010.
- [107] Park, B. Y., Taherabadi, L., Wang, C., Zoval, J., Madou, M. J., *J Electrochem Soc* 2005, *152*, J136-J143.
- [108] Siegel, A. C., Tang, S. K., Nijhuist, C. A., Hashimoto, M., Phillips, S. T., Dickey, M. D., Whitesides, G. M., *Acc Chem Res* 2010, *43*, 518-528.
- [109] So, J.-H., Dickey, M. D., *Lab Chip* 2011, *11*, 905.

- [110] Niu, X. Z., Peng, S. L., Liu, L. Y., Wen, W. J., Sheng, P., *Adv Mater* 2007, *19*, 2682-2686.
- [111] Gong, X., Wen, W., *Biomicrofluidics* 2009, *3*, 012007.
- [112] Niu, X., Zhang, M., Peng, S., Wen, W., Sheng, P., *Biomicrofluidics* 2007, *1*, 044101.
- [113] Lewpiriyawong, N., Yang, C., Lam, Y. C., *Electrophoresis* 2010, *31*, 2622-2631.
- [114] Deman, A. L., Brun, M., Quatresous, M., Chateaux, J. F., Frenea-Robin, M., Haddour, N., Semet, V., Ferrigno, R., *J Micromech Microeng* 2011, *21*, 095013.
- [115] Spadaro, J. A., Berger, T. J., Barranco, S. D., Chapin, S. E., Becker, R. O., *Antimicrob Agents Chemother* 1974, *6*, 637-642.
- [116] Zhu, Z. Y., Zhang, F. Q., Xie, Y. T., Chen, Y. K., Zheng, X. B., *Mater Sci Forum* 2009, *620-622*, 307-310.
- [117] Choi, J.-W., Rosset, S., Niklaus, M., Adleman, J. R., Shea, H., Psaltis, D., *Lab Chip* 2010, *10*, 783.
- [118] Cheung, K., Gawad, S., Renaud, P., *Cytom Part A* 2005, *65A*, 124-132.
- [119] Mernier, G., Piacentini, N., Braschler, T., Demierre, N., Renaud, P., *Lab Chip* 2010, *10*, 2077-2082.
- [120] Boettcher, M., Jaeger, M., Kirschbaum, M., Mueller, T., Schnelle, T., Duschl, C., *Anal Bioanal Chem* 2007, *390*, 857-863.
- [121] Gomez-Quiñones, J., Moncada-Hernandez, H., Rosetto, O., Martinez-Duarte, R., Lapizco-Encinas, B. H., Madou, M., Martinez-Chapa, S. O., *Proceedings of IEEE New Circuits and Systems Conference (NEWCAS)* 2011, 350-353.

TABLES

Table 1 This table reflects the different fabrication processes and materials so far used, and published, in different DEP techniques. Other materials and fabrication processes may be used to achieve the same results. The cost column is a comparison between the different techniques: \$ = less expensive. Representative processes for the fabrication of a microfluidics network for each technique are included in the last column. Please note that in some cases an “open” microfluidics network, channels and chambers, is fabricated simultaneous with the insulator structures or electrodes. However, additional techniques, such as anodic bonding, or materials, such as adhesives or glue, are needed to close and seal the microfluidic network.

DEP Technique		Fabrication Processes ^{\$}	Materials	3D?	Cost	Fabrication of supporting microfluidics
Metal-electrode		Metal deposition Polymer mask [#] Metal etching ^{&}	Photoresists, glass or plastic substrate, thin film Au, Pt, Al or other metals as electrodes; ITO commonly used for planar transparent electrodes	No, if using planar electrodes	\$\$\$	- Casting of a PDMS part followed by plasma activation and later positioning on top of the electrodes. - Photolithography of a polymer layer on top of the electrodes. Photoresist deposited by spin coating or dry film lamination. Device closed using glass or polymer substrate and adhesive or glue (<i>i.e.</i> UV, epoxy-based)
		+ Electroplating, if making 3D structures		Yes, if using electroplating	\$\$\$\$	
Doped Silicon		Metal deposition Polymer mask Metal etching Silicon etching (DRIE)	Photoresists, thin film metal, doped silicon, glass	Yes	\$\$\$\$	µm-scale fluidics made together with the silicon electrodes. Network is closed using a glass lid and anodic bonding.
I N S U L A T O R - B	Insulator matrices	Dispensing of dielectric beads Machining, cutting to pattern macro electrodes	Plastics, dielectric beads (most commonly glass), stainless steel or other metal pieces/foils	Yes	\$	mm-scale fluidics done by machining, molding, etc. Device closed using glass or plastic substrate and adhesive, glue or solvent-assisted
	Insulator structures – metal macro electrodes	Glass-based devices: Metal deposition Polymer mask Metal etching Glass wet etching	Photoresists, thin film metal, float glass (quartz has also been used), metal wire	Yes	\$\$\$\$	µm-scale fluidics done together with the glass micro-structures. Network is closed using a glass lid and anodic bonding.
		Polymer-based devices: Molding or Embossing and/or Machining	Polymer, metal wire, pieces or foil	Yes	\$\$	Concurrent fabrication with the insulator structures. Closed by a polymer lid and adhesives, glue or solvent-assisted

A S E D	Contactless (co-fabrication)	Casting + Mold fabrication: polymer mask, silicon etching (DRIE)	PDMS, metal wire, glass substrate + photoresists, and silicon	Yes	\$\$	μ m-scale fluidics to hold sample and conductive liquids fabricated together. PDMS part sealed against a glass or plastic substrate after plasmaactivation
	Insulator-structures – metal micro electrodes	Metal deposition Polymer mask Metal etching Thick-film photolithography [#]	Photoresists, Au, ITO, glass or plastic substrate	Yes	\$\$\$	Photolithography of a spin-coated polymer layer. Device closed using glass or polymer substrate and adhesive, glue or solvent-assisted
Liquid-electrode	Metal deposition Polymer mask Metal etching Photolithography	No		Network done together with the SU-8 layer enabling the “liquid-electrode” concept. Device closed before each experiment using a PDMS part and mechanical pressure		
Light-induced	Deposition	ITO, amorphous silicon, glass or plastic substrate	No	\$\$	Basic fluidic chambers using adhesive or polymer spacers	
Carbon-electrode	Thick-film photolithography Pyrolysis	Photoresists, fused silica or silicon substrate	Yes	\$\$	Sub mm-scale network cut in double-sided adhesive. Stack of adhesive and drilled plastic sealed around electrode array using rolling press	
Liquid metal (co-fabrication)	Casting Metal injection + Mold fabrication: photolithography	Glass substrate, PDMS, liquid-phase or low melting point metals + photoresists	Yes	\$\$	μ m-scale fluidics to hold sample and cavities for metal injection fabricated together. PDMS part sealed against a glass or plastic substrate after plasmaactivation	
Doped PDMS	Casting Mixing + Mold fabrication: photolithography	Conductive particles, PDMS, glass substrate + photoresists	Yes	\$\$	μ m-scale fluidics fabricated in the pure PDMS part. The PDMS-Doped PDMS part is then sealed against a glass or PDMS substrate after plasmaactivation	
	Casting + Mold fabrication: photolithography + Metal ion	PDMS, Au, ITO, glass substrate		\$\$\$	μ m-scale fluidics fabricated in the PDMS part that is later implanted with metal ions. Metal-implanted PDMS part is sealed	

	implantation, metal and ITO patterning,				against the ITO-coated glass substrate after plasmaactivation
--	---	--	--	--	---

Notes:

§ Cleaning of the substrate previous to fabrication is not included here as all processes require it. Effective cleaning can be done using a piranha bath (3:1 H₂SO₄(concentrated):H₂O₂(30%)), if the material allows it, or oxygen plasma treatment. Milder treatments such as cleaning with solvents like isopropyl alcohol may be enough in some cases.

Polymer mask refer to the patterning of a polymer layer to be used as mask for metal etching or lift-off, or silicon etching; the process includes photolithography of a photoresist, usually a positive-tone one, and polymer stripping. In this table, polymer mask is different from photolithography in that the latter is usually done to fabricate structures, most commonly in negative photoresists, that will remain on the experimental device.

& Metal etching is not necessary if lift-off techniques are used. Alternatively, metal patterning can be done directly by using laser ablation or ion-milling instead of the combination of a polymer mask and wet or dry metal etching.

FIGURES

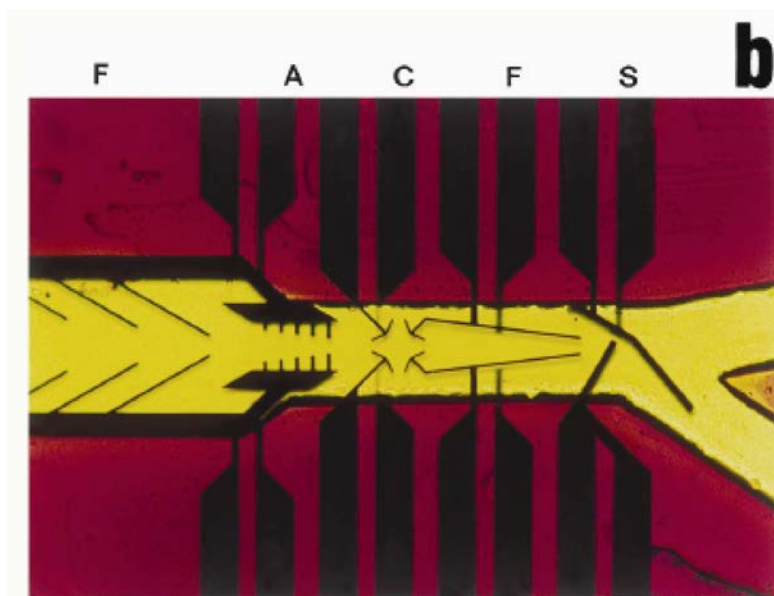


Figure 1. A DEP chip featuring aligned electrodes on the bottom and ceiling of a microfluidic channel (bright region). The channel is 40 μm high. Different functions are implemented such as funneling (F), aligning (A), trapping in an octopole cage (C) and sorting using a switch (S). Reprinted from [38] with permission from Elsevier.

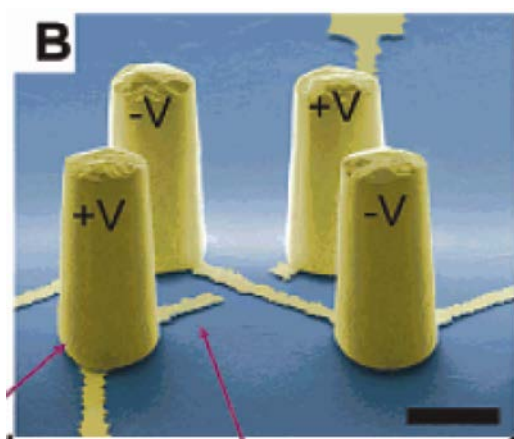


Figure 2. Left: Pseudocolored scanning electron micrograph showing a single quadrupole trap consisting of four electroplated gold electrodes arranged trapezoidally along with the substrate interconnects. The scale bar represents 20 μm . Reprinted with permission from [40]. Copyright 2002 American Chemical Society.

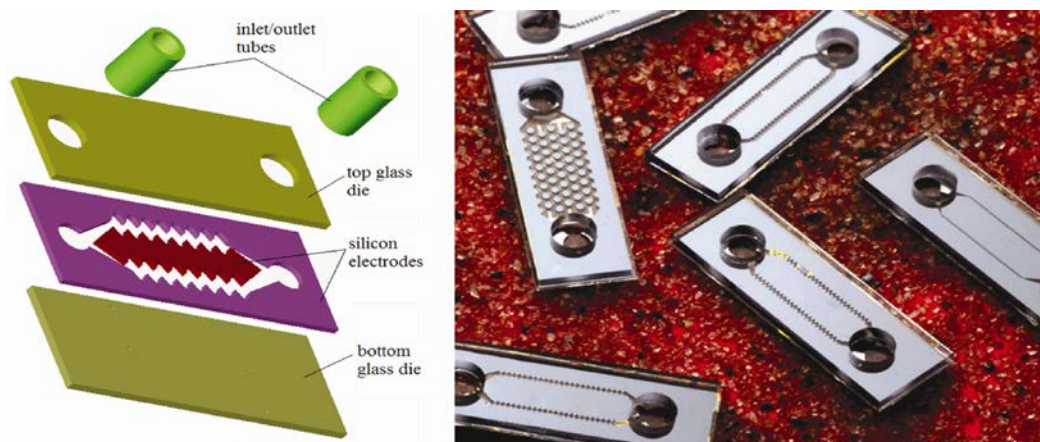


Figure 3. Left: Schematic of the parts forming a doped silicon-based DEP device. Right: experimental devices featuring different designs. Courtesy of Ciprian Iliescu.

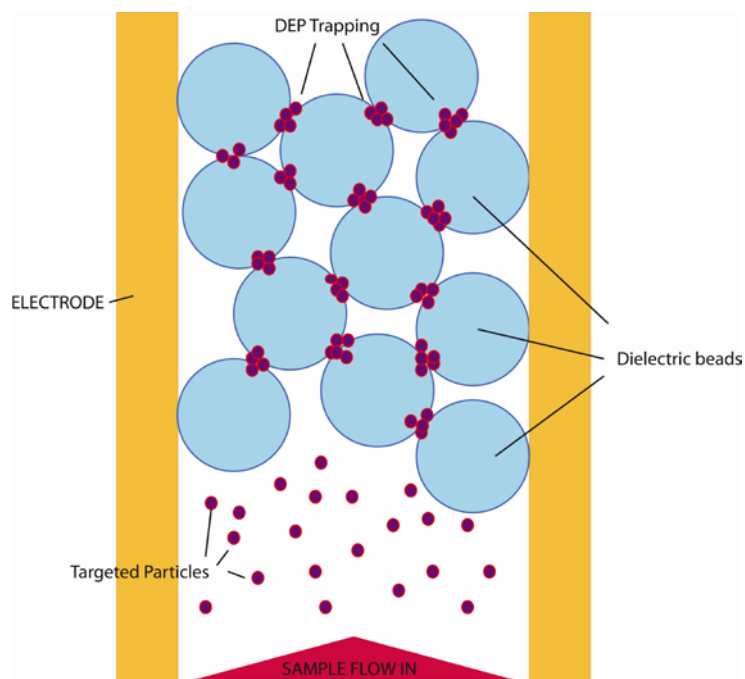


Figure 4. Dielectric beads packed in between electrodes. The targeted cells are trapped against a liquid flow (sample flow in) at the regions of high electric field gradient, in this case on the contact points between beads.

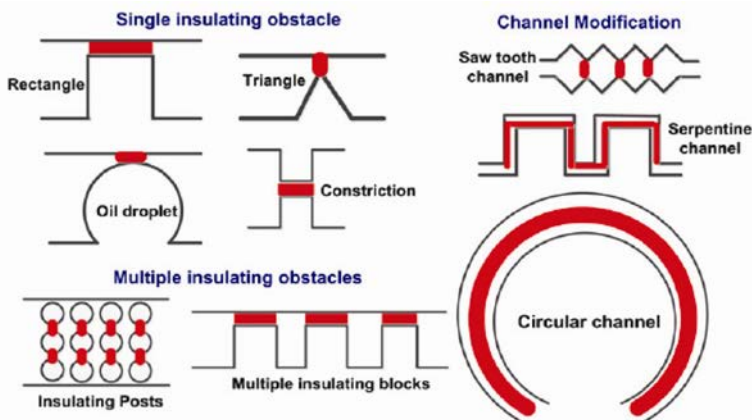


Figure 5. Different insulating geometries so far demonstrated for the DEP manipulation of particles. With kind permission from Springer Science + Business Media: Anal Bioanal Chem, DC insulator dielectrophoretic applications in microdevice technology: a review, volume 399, 2010, Srivastava S. K. and Minerick, A., Figure 4.

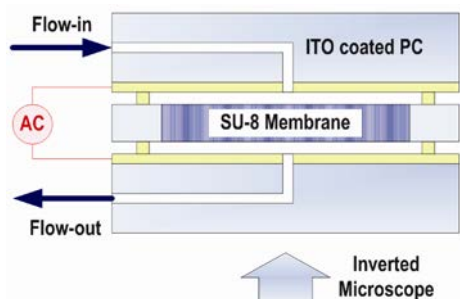


Figure 6. A SU-8 membrane used as a DEP-active filter. The membrane is positioned in between a couple of planar electrodes (ITO-coated polycarbonate). Upon polarization of the planar electrodes, bacteria cells are trapped in the electric field gradients formed at the edge of the pores in the membrane. Reprinted from [74] with permission from John Wiley and Sons.

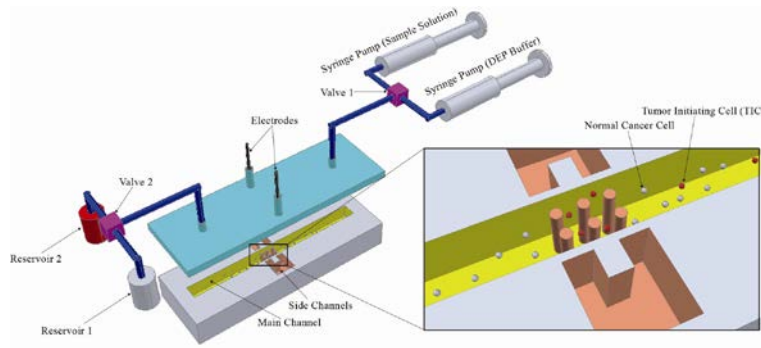


Figure 7. Schematics of a contactless Dielectrophoresis device. A main channel (yellow) is coupled to side channels (grey) using a very thin membrane. After fabrication, the side channels are filled with a conductive liquid. An electric field gradient is created in the main channel, around the thin membrane, upon polarizing the now conductive side channels using wire electrodes. Courtesy of Hadi Shafiee and Rafael Davalos.

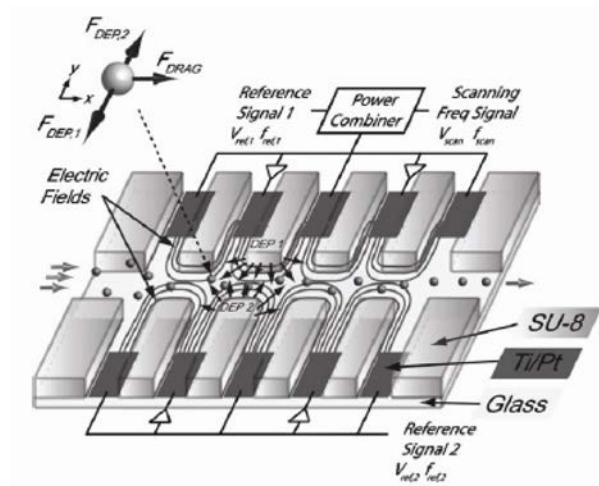


Figure 8. 3D schematic of a “liquid electrode” DEP device. SU-8 side channels are patterned on top of planar metal electrodes. These distant metal electrodes are used to generate an electric field inside the central fluidic channel where the particles flow. Single or combined signals applied to the electrodes create two opposite DEP forces across the central channel. Reprinted from [82] with permission from Elsevier.

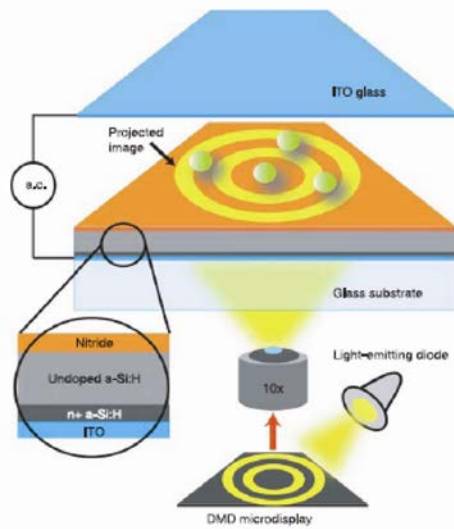


Figure 9. A light-induced DEP device. A photoconductive layer featuring amorphous silicon is patterned on top of a transparent electrode. A second electrode is placed on top, spaced by tens of micrometers. An AC signal is used to polarize both electrodes to create a uniform electric field. Field gradients are introduced when a light pattern is shone on the photoconductive layer, thus creating virtual electrodes (the bright concentric rings). Reprinted by permission from Macmillan Publishes Ltd: Nature [97], copyright 2005.

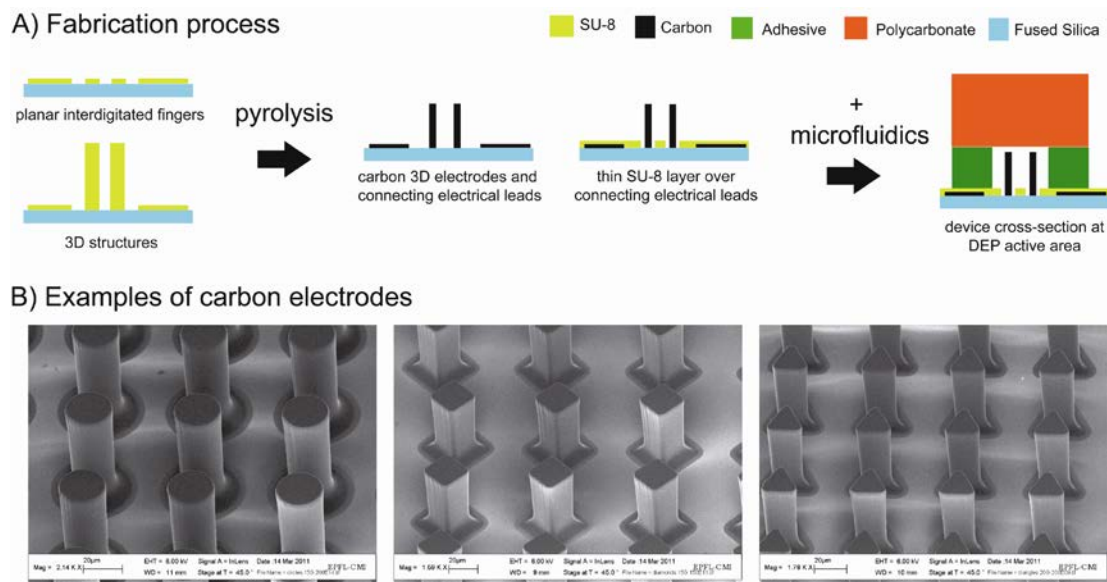


Figure 10. Fabrication process of a carbon-electrode DEP device and examples of different carbon electrode geometries. A polymer precursor is patterned and then carbonized by pyrolysis at 900 °C in an inert atmosphere. The microfluidic network is made by stacking patterned

double-sided adhesive and polycarbonate pieces. Reprinted from [104] with permission from John Wiley and Sons.

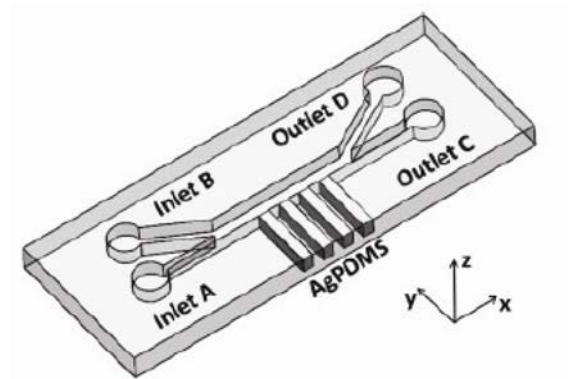


Figure 11. A DEP device featuring doped PDMS electrodes embedded on the walls of a channel, also fabricated on PDMS. Silver-doped PDMS is shown in this case. Cells injected into the chip can be selectively deflected to outlet D or C depending on the signal polarizing the AgPDMS electrodes. Reprinted from [113] with permission from John Wiley and Sons.

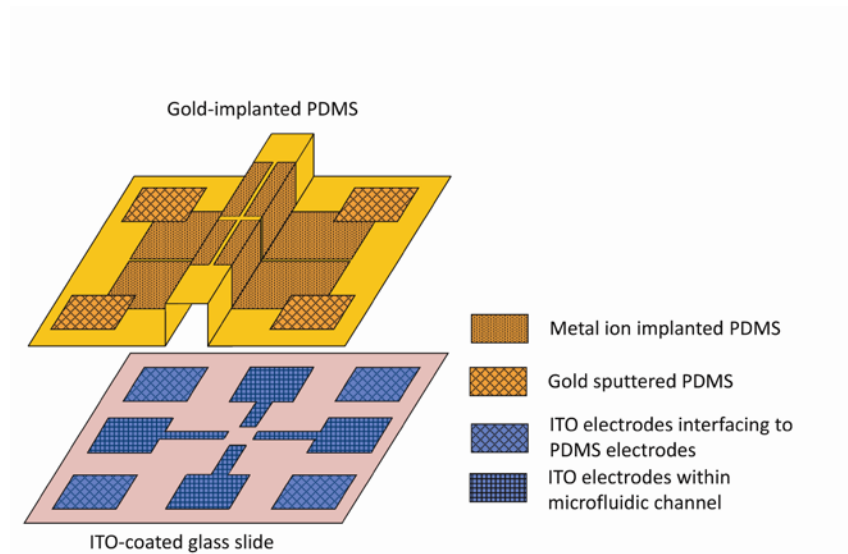


Figure 12. An octopole DEP trap fabricated by implanting gold on the side walls of a PDMS channel and bonding such PDMS piece to previously patterned ITO electrodes on a glass slide. Courtesy of Jae-Woo Choi.